CrystEngComm

PAPER

View Article Online
View Journal

Cite this: DOI: 10.1039/c8ce00855h

A chiral spiroborate anion from diphenyl-L-tartramide $[B\{L\text{-}Tar(NHPh)_2\}_2]^-$ applied to some challenging resolutions†

Lawrence W.-Y. Wong, Gemma S.-S. Tam, Xiaoyan Chen, Frederick T.-K. So, Aristyo Soecipto, Fu Kit Sheong, Herman H.-Y. Sung, Zhenyang Lin and Ian D. Williams *

The chiral spiroborate anion $[B\{L\text{-}Tar(NHPh)_2\}_2]^-$ has been prepared as simple salts K, NH_4, Na in high yield and purity. Its structural features have been examined by single crystal XRD and DFT calculations and indicate that conformational arrangements are dominated by intramolecular NH---O=C inter-amide hydrogen bonds. These confer predictable shape, as well as a clear binding site for ion-pair formation. The potential of this anion for resolution by diastereomeric salt formation was then tested using five challenging racemic amines of type $NH_2CHR_1R_2$ with high shape similarity between their enantiomers. Organoammonium salts from these were made directly from a simple 1-pot reaction from racemic amine, boric acid and 2 eq. *N,N′*-diphenyl-L-tartramide in MeOH. The products are single phase crystalline solids with moderate to excellent enantioexcesses up to 95% ee. They show conserved NH_3R^+ binding and layered packing arrangements, all with short 5.5 Å axes. Based on chiral HPLC the initial $[B\{L\text{-}Tar(NHPh)_2\}_2]$ salt from *rac*-phenylglycinol has $[S\text{-}NH_3CH(CH_2OH)Ph]^+$ with 95% ee and the salt from *rac*-1-phenylpropylamine is also well resolved (>91% ee) in a single step. Three disorder modes that limit resolution in the other salts were identified at the cation site – H/R_1 site exchange, R_1/R_2 site exchange or C–H re-pyramidalization. Extension to a family of such aryltartramide anions may allow crystal engineering of the cation binding pockets to overcome the disorder inherent to such resolutions.

Received 23rd May 2018,
Accepted 12th July 2018

DOI: 10.1039/c8ce00855h

rsc.li/crystengcomm

Introduction

The separation of enantiomers from a racemate *via* selective diastereomeric crystallization[1,2] is a classical optical resolution method of considerable value to pharmaceutical and chemical industry[3] that can benefit from the application of modern crystal engineering approaches.[4] In the case of salts a pure enantiomer of one ion is introduced to a racemic mixture of counterions with the idea that two diastereomeric salts may be formed with differing physical properties and solubility. Ideally the less soluble salt will be selectively precipitated, removing one hand of the racemic ion to the solid whilst leaving the other in solution. By judicious selection of resolving ion, solvent and other conditions highly efficient resolutions can be achieved by this approach.[4]

Several factors can affect the effectiveness of resolving ions, shape, size, functionality, degree of chirality. They should form crystalline solids with a wide range of counterions and have low tendency for disorder. From a practical viewpoint ideally they should also be inexpensive, non-toxic, unreactive and readily available in both hands. Recently we described the use of the chiral spiroborate anions bis(mandelato)borate $[B(R\text{-}Man)_2]^-$ and $[B(S\text{-}Man)_2]^-$ as promising and versatile resolving agents that meet the above criteria.[5] Resolutions could be carried out by one-pot procedure, or they can be readily prepared and isolated as simple salts, such as $Na[B(R\text{-}Man)_2]$, that could then be used in a metathesis crystallization.[6] Examples included resolution of the alkaloid base tetrahydropalmatine as its monoprotonated cation $(THP\text{-}H)^+$, the simple diamine 1,2-diaminopropane as its di-ammonium salt $[1,2\text{-}dap\text{-}H_2]^{2+}$ and the metal coordination complex tris-phenanthroline cobalt^{III} $[Co(phen)_3]^{3+}$.[5]

A single anion such as $[B(Man)_2]^-$ cannot guarantee success in a specific diastereomeric salt system, so a larger collection of resolving agents[7] is needed for improving the chances of a successful, efficient resolution. Spirocompounds are privileged chiral architectures,[8] so we sought to build on our earlier $[B(Man)_2]^-$ results and develop a

Department of Chemistry, Hong Kong University of Science and Technology, Clear Water Bay, Kowloon, Hong Kong, China. E-mail: chwill@ust.hk; Fax: +852 2358 1594; Tel: +852 2358 7384

† Electronic supplementary information (ESI) available: Single crystal structure determination summaries, powder X-Ray Diffractograms, chiral HPLC chromatograms and other spectra. CCDC 145865–145868 and 1844600–1844603. For ESI and crystallographic data in CIF or other electronic format see DOI: 10.1039/c8ce00855h

wider family of spiroborate anions. Whilst both enantiomers of mandelic acid itself are inexpensive and readily available in bulk quantity, most of its derivatives are not. To form a family of spiroborate anions we sought a set of chiral chelating oxyacid-ligands that could be readily prepared. They should allow incorporation of functional groups to enable crystal engineering of diastereomeric salts at the molecular level.

Tartramides are a class of chiral diols that appear ideally suited to this need.[9] They can be readily prepared by a single step from cheap L-tartaric acid (or the unnatural D-form which is also inexpensive) with a wide range of amines and their bis-chelation to boron (Fig. 1) should form a family of chiral spiroborate anions.

Sharpless' asymmetric epoxidation method was based on the use of titanium tartrate-ester and tartramide catalysts.[10] Toda *et al.* also successfully applied chiral tartramides as hosts for resolution by inclusion complexation.[9] Furthermore coordination of tartrate by antimony^{III} affords dimeric anions with good resolving power,[11] so it is reasonable that bis(tartramido)borate anions $[B\{Tar(NR_2)_2\}_2]^-$ might also have promise as resolving agents.

In this paper we begin to explore this possibility through synthesis of a prototype chiral anion $[B\{L\text{-}Tar(NHPh)_2\}_2]^-$ derived from *N*,*N*′-diphenyl-L-tartramide, conveniently synthesized from condensation of aniline with L-tartaric acid. First the preparation and structure of simple salts of $[B\{L\text{-}Tar(NHPh)_2\}_2]^-$ is described. (Fig. 1) The spiroborate anion is then deployed in the attempted resolution of five racemic amines of the type $NH_2CHR_1R_2$, *sec*-butylamine (R_1 = Me, R_2 = Et), 2-pentylamine (R_1 = Me, R_2 = Et), 2-phenylethylamine (R_1 = Me, R_2 = Ph), 2-phenylpropylamine (R_1 = Et, R_2 = Ph) and phenylglycinol (R_1 = CH_2OH, R_2 = Ph). These systems provide a challenge to resolution by the diastereomeric salt method, since their enantiomers have considerable shape similarity.[12] This means they may form diastereomeric mixed crystals[13] or solid solutions[14] – single phase products with disorder of the enantiomers at the cation sites. These may necessitate multistage recrystallizations to achieve acceptable enantiopurity.[15] The success and limitation of the diphenyltartramide spiroborate anion to such resolutions and the modes of disorder found in its diastereomeric chiral ammonium salts will be discussed.

Results and discussion

Simple spiroborate salts from $[L\text{-}Tar(NHPh)_2\text{-}H_2]$

The chiral diol *N*,*N*′-diphenyl-L-tartramide **1** (Fig. 1) $[L\text{-}Tar(NHPh)_2\text{-}H_2]$ was chosen as a starting ligand, since it was readily prepared from L-tartaric acid and aniline and was previously used as a chiral host for guest-host complex formation by Toda *et al.*,[9] to achieve the resolution of axially chiral *bis*-phenols such as BINOL.[16] Our initial goal was to show that chiral spiroborate anions could be readily formed from **1** and crystallize them as salts to explore their structural chemistry and potential for resolution.

Ideally the $[B\{L\text{-}Tar(NHPh)_2\}_2]$ anion could then serve as a prototype for an extensive family of spiroborates, since a wide range of tartramide diols are accessible by varying the aniline or amine used in the condensation with tartaric acid.

As with bis(mandelato)borate $[B(Man)_2]^-$,[5,6] our approach was to prepare the spiroborate first as an alkali metal salt by direct 1-pot reaction of KOH, boric acid and 2 eq. of the chelating oxy-acid, in this case the diol **1**, as shown schematically in Fig. 1. The use of lower temperatures and reaction times and non-solvothermal conditions can be applied to this synthesis, but the solvothermal conditions we use tend to give suitably crystalline and phase pure products in a single step. They also avoid the tendency to gel formation that have been frequently encountered in such systems, perhaps due to 1D coordination or H-bond chains in these salts.[17,18]

In the case of potassium, the desired salt $K[B\{L\text{-}Tar(NHPh)_2\}_2]$ **2** is formed in good yield and purity as platy crystallites by solvothermal crystallization in MeOH at 110 °C for 1 day. A small micro-crystallite of **2** was chosen for single crystal structure determination. The phase is monoclinic with chiral space group *C*2 and was found to be a non-solvated form of the compound. Overall the asymmetric unit contains one formula unit, but has two separate K^+ cations and two spiroborate $[B\{L\text{-}Tar(NHPh)_2\}_2]^-$ anions that all sit on crystallographic 2-fold axes. A symmetry generated ion-pair based on K(1) and B(1) is depicted in Fig. 2a, a similar geometry is found for the K(2) and B(2) ion-pair. In principle a $[B\{L\text{-}Tar(NHPh)_2\}_2]^-$ anion should have four chemically equivalent arms, however an intra-ligand NH---O=C hydrogen bond (N(1)–H(1)---O(4) = 3.061(3)Å) is formed between the two arms of each ligand, rendering the chelating diolate asymmetric.

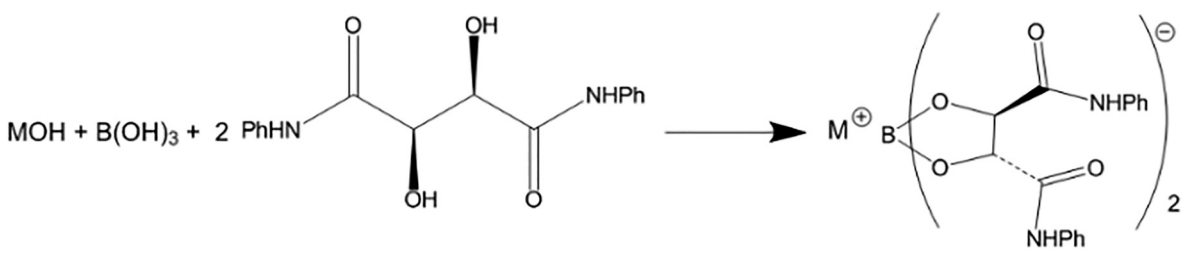

Fig. 1 Synthetic scheme for simple bis(diphenyltartramido)borate salts M = K, NH_4, Na (**2**–**4**). Use of *rac*-amines as base allows extension of this to preparation of organoammonium salts (**5**–**9**).

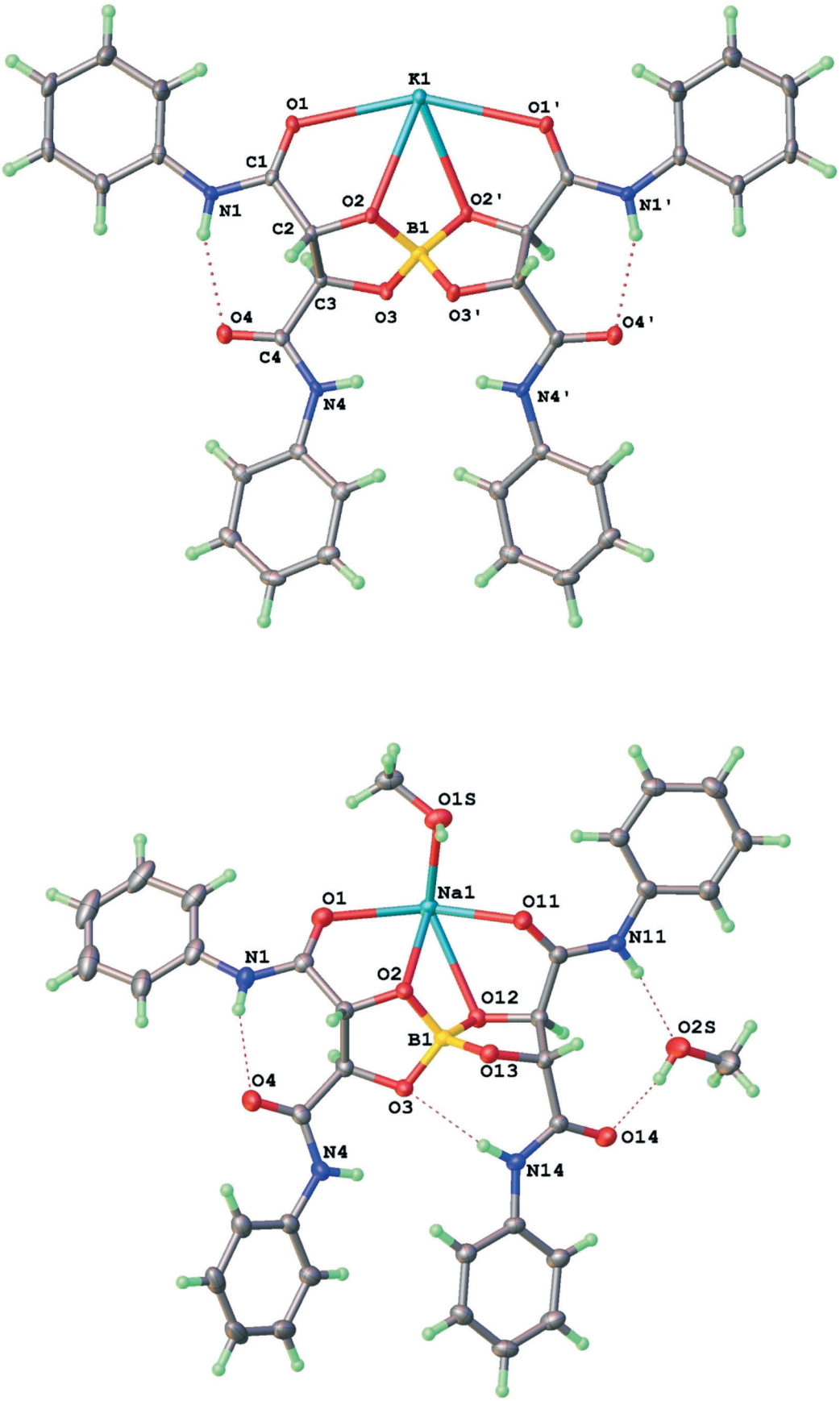

Fig. 2 a) Structure of ion pair K[B{L-Tar(NHPh)$_2$}$_2$] in **2**,and b) Na salt **4**, 50% probability ellipsoids.

Intriguingly this asymmetry of chelation then nominally introduces a stereochemical center at boron. If the NH donor side is taken as higher priority substituent this gives a B_S-stereochemical center (this still holds if the reverse priority is assigned, since both ligands are affected by the change).

The projection of the spiroborate anion in Fig. 2a has the Ph groups disposed in what could be loosely called a "Y-shape". Another conformational possibility chelating the second Tar(NHPh)$_2$ the other way around gives a B_R-configuration which has Ph group disposition more like an "X-shape" for the same projection (for further discussion, see below and Fig. 11). In our recent studies of bis(mandelato)borate [B(Man)$_2$]$^-$ anions diastereomeric conformations described as "Twisted" and "V-shaped" resulted from B_R- and B_S-stereochemistry with S-mandelate ligands respectively.[5] The gas phase or solution energies of the two quite different shapes were shown to be energetically similar and hence likely to have similar solution populations, although only the "Twisted" conformational anions were found in the solid state.

In the case of bis(*N*,*N*′-diphenyltartramido)borate [B{L-Tar(NHPh)$_2$}$_2$]$^-$ it is worth noting that the 'asymmetry' of the ligand is not fixed as is the case of mandelate, but could dynamically switch with amide rotation with concomitant breaking and possible re-formation of intramolecular NH---OC amide H-bonds. This would scramble the ligand asymmetry and hence the 'boron stereochemistry' without any need for disruption of the actual boron BO_4 tetrahedral arrangement itself.

As shown in Fig. 2a K(1) sits in a pocket of four contacts to O(1), O(2), O(2)′ and O(1)′ where the primes are the 2-fold related atoms. The K(1) also makes two separate chelations to the B(2) based anions coordinating the diolate O(2) and O(3) type-oxygen atoms, so that overall K(1) is eight coordinate. A similar arrangement is found for K(2) and which coordinates a tetradentate pocket for the B(2) anion and makes single chelations to O(2) and O(3) for two B(1)-based anions. Overall the K^+ and [B{L-Tar(NHPh)$_2$}$_2$]$^-$ anions form a 1D molecular stack along the [001] direction, (see Fig. S1†). The molecular stack interdigitates its Ph rings with those of other neighboring stacks to provide the overall 3D crystal structure. In addition to NH---O H-bonds between different halves of the same ligand there are also incipient H-bond contacts N(4)–H(4)---O(3) = 2.630 Å, although the angle at H is just 113.9°. Despite the fact that [B{L-Tar(NHPh)$_2$}$_2$]$^-$ has a tetrahedral arrangement at boron one effect of the intramolecular H-bonds is that the molecular anion is flattened into a corrugated planar shape.

Using related solvothermal synthetic conditions to the formation of **2**, the substitution of NH_4OH gave an isostructural phase type [NH_4][B{L-Tar(NHPh)$_2$}$_2$], **3**. The X-ray structure clearly showed the H-bond arrangement between the ammonium and spiroborate ions and is instructive in seeing how there is a similar cation recognition site for ammonium H-bonding to the anion similar to the tetradentate coordination site for potassium.

The substitution of NaOH into the reaction scheme in Fig. 1 gives the salt Na[B{L-Tar(NHPh)$_2$}$_2$] **4**, this time as a di-methanolate phase. Variation of conditions (time and temperature) within the methanol system did not result in formation of an unsolvated phase and a change of solvent typically afforded a hydrated phase instead. The di-methanolate **4** is quite reproducibly prepared, phase pure and the resulting crystal structure of reasonable quality. Crystals of **4** are orthorhombic with the $P2_12_12_1$ space group. The asymmetric unit contains one formula unit and the Na[B{L-Tar(NHPh)$_2$}$_2$] ion pair and two methanols, as shown in Fig. 2b.

The structure of **4** exemplifies how the structure of the [B{L-Tar(NHPh)$_2$}$_2$]$^-$ anions can be modified by solvation. One MeOH coordinates to the Na while the other MeOH is 'inserted' into an amide NH---O H-bond, thus slightly modifying the anion's conformational shape. The Na^+ cation again sits in a tetradentate pocket of the anion formed by O(1) O(2) O(12) and O(11) in a similar way to K ion in **2**. The smaller Na is coordinated to MeOH and a single bidentate chelation to a neighboring [B{L-Tar(NHPh)$_2$}$_2$]$^-$ through the O(2)–O(13) edge of the BO_4 tetrahedron.

The N(1)–H---O(4) H-bond is still in place on one half of the ion but on the second half the H-bond arrangement is more extended so that a second uncoordinated methanol acts as acceptor from NH and donor to amide C═O, N(11)–H---O(2S)–H---O(14). The result of this is that the fourth arm swings around and forms a N(14)–H---O(3) hydrogen bond of 3.083 Å between the two ligands. The [B{L-Tar(NHPh)$_2$}$_2$]$^-$ anion in **4** thus has a slightly modified shape from the K salt **2**, as seen in the overlay in Fig. 3. Despite the change introduced by the smaller sodium and insertion of solvent in modifying the NH---O═C amide hydrogen bonding an overall conformational preference for [B{L-Tar(NHPh)$_2$}$_2$]$^-$ anion begins to emerge. A similar 'semi-rigid' structure was noted for

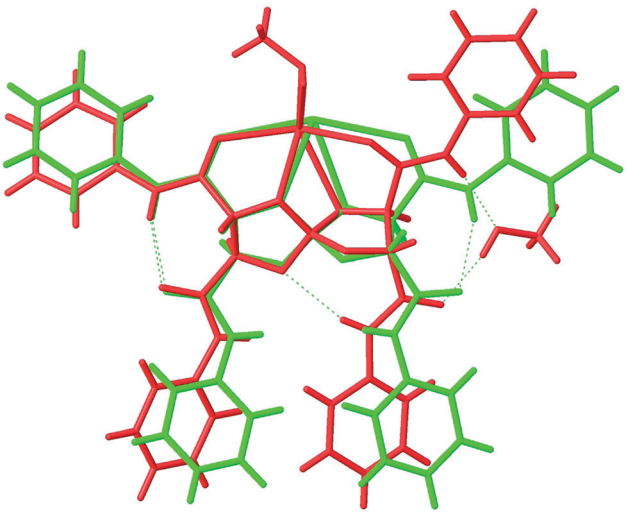

Fig. 3 Overlay of K[B{L-Tar(NHPh)$_2$}$_2$] **2** (pale green) and Na[B{L-Tar(NHPh)$_2$}$_2$]·2MeOH, **4** (dark red) showing effect of MeOH 'insertion' on spiroborate conformation.

$[B(Man)_2]$ ions[5] and deemed helpful in providing crystalline products with a wide range of counterions.

Application of chiral anion $[B\{L\text{-}Tar(NHPh)_2\}_2]^-$ to resolution

In order to test whether $[B\{L\text{-}Tar(NHPh)_2\}_2]^-$ could achieve a similar chiral discrimination to $[B(Man)_2]^-$, we next attempted to employ the bis(diphenyltartramido)borate anion in resolution of five racemic amines, *sec*-butylamine ($NH_2CHMeEt$) and 2-pentanamine ($NH_2CHMePr$) as well as 1-phenylethylamine($NH_2CHMePh$), 1-phenylpropylamine($NH_2CHEtPh$) and 2-phenylglycinol ($NH_2CH(CH_2OH)Ph$). These were chosen to be challenging since there is a single chiral center with a strong shape similarity between the enantiomers of each racemic pair. Consequently, the resolution needs to discriminate not only through distinct solubilities of pure diastereomeric salts, but also in limiting possible cation site disorder in single phase *solid-solutions*. As will be seen three main classifications of such site disorder can be considered in these systems, as shown in Fig. 4.

Resolutions with varying degrees of success have been achieved for *sec*-butylamine from diastereomeric salts of deoxycholic acid[19] and tartaric acid[20] or by neutral molecule cocrystallization.[21] The case of *rac*-1-phenylethylamine(α-methylbenzylamine) is slightly less demanding and has been previously resolved using mandelic[22] and tartaric acids.[23] Subsequently its enantiomerically pure forms have become standard resolving cations in their own right[24] and some of its diastereomeric salts have been the subject of computational studies to aid rational design of resolving agents.[25] Our previous efforts to employ $[B(Man)_2]^-$ in the resolution of the two racemic bases *sec*-butylamine and 1-phenylethylamine met with limited success,[26] so they offer an exacting challenge for potential new chiral spiroborate anions.

First the feasibility of resolution of racemic *sec*-butylamine ($NH_2CHMeEt$) was attempted through a direct 1-pot solvothermal crystallization, similar to that of simple salts **2–4**, only employing the *rac*-amine as the base. As a strategy to optimize % ee in a precipitated diastereomeric salt Fogassy suggests to use only 50 mol% of the racemic ion in a resolution,[27] with a possible addition of a more soluble achiral counter-ion to retain the unwanted enantiomer in solution.[28]

In practice we have found that acceptable results were obtained for $[BMan_2]$ by using a stoichiometric amount of racemic cations for the chiral anion used, so made initial reactions in this way with the idea that ratios and conditions could later be varied to optimize yield and % ee in the resulting solids.

Like the K salt **2**, the product crystals $[R/(S)\text{-}NH_3CHMeEt][B\{L\text{-}Tar(NHPh)_2\}_2]$ **5** are unsolvated and belong to the orthorhombic system with chiral space group $P2_12_12_1$. The asymmetric unit consists of an ion pair as shown in Fig. 5a. We use the R/(S)-nomenclature to indicate the cation is predominantly R-configuration. The cation site is disordered with a best fit indicating about a 67 : 33 ratio of the R-cation to its S-enantiomer. Interestingly it is not C–H/C–Me disorder at the chiral carbon center, but C–Me/C–Et disorder that causes the loss of enantiospecificity. The packing in **5** is shown in Fig. 10 and reveals the 2_1 screw of cations are in close contact with each other. The disordering of R- and S-cations may be partially due to the possibility of mutual cation disordering due to the fact that the cation neighbors are in contact with each other in their aliphatic regions.

Whilst variations in crystallization conditions could probably improve on the initial 34% ee found, the packing implies that for this phase a usefully high level of chiral discrimination is unlikely. Several other solvents were used to see whether a change of phase type could be induced with superior resolution characteristics, but various other alcohols and polar solvents such as acetonitrile and acetone yielded either the same phase type **5**, or poorly crystalline/gel like products.

The resolution for *sec*-butylamine of an approximately 2 : 1 ratio of R : S cations in the salt prepared from the racemic amine in a 1-pot reaction still represents a modest success given the extreme similarity of the enantiomeric organoammonium ions. The observed R_1/R_2 disorder of the Me and Et positions is hard to mitigate against. It was decided to probe this issue further by perturbing the racemic amine and study the related 2-pentylamine. In this case the Et group at the chiral centre is replaced with slightly larger ^{n}Pr. The chiral coefficient of this amine is slightly larger and it seemed reasonable that a Me/Pr disorder would be less likely. The crystallization of the corresponding organoammonium salt $[NH_3CHMePr][B\{L\text{-}Tar(NHPh)_2\}_2]$ **6** was carried out in similar

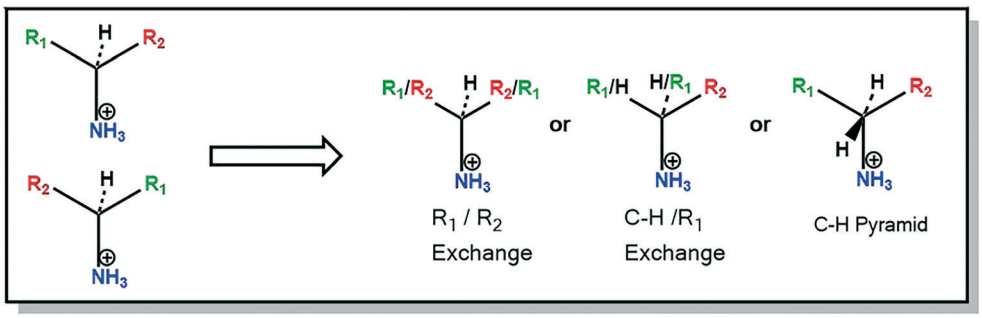

Fig. 4 Three distinct disorder modes that have been identified at the cation sites in the organoammonium salts **5–8**.

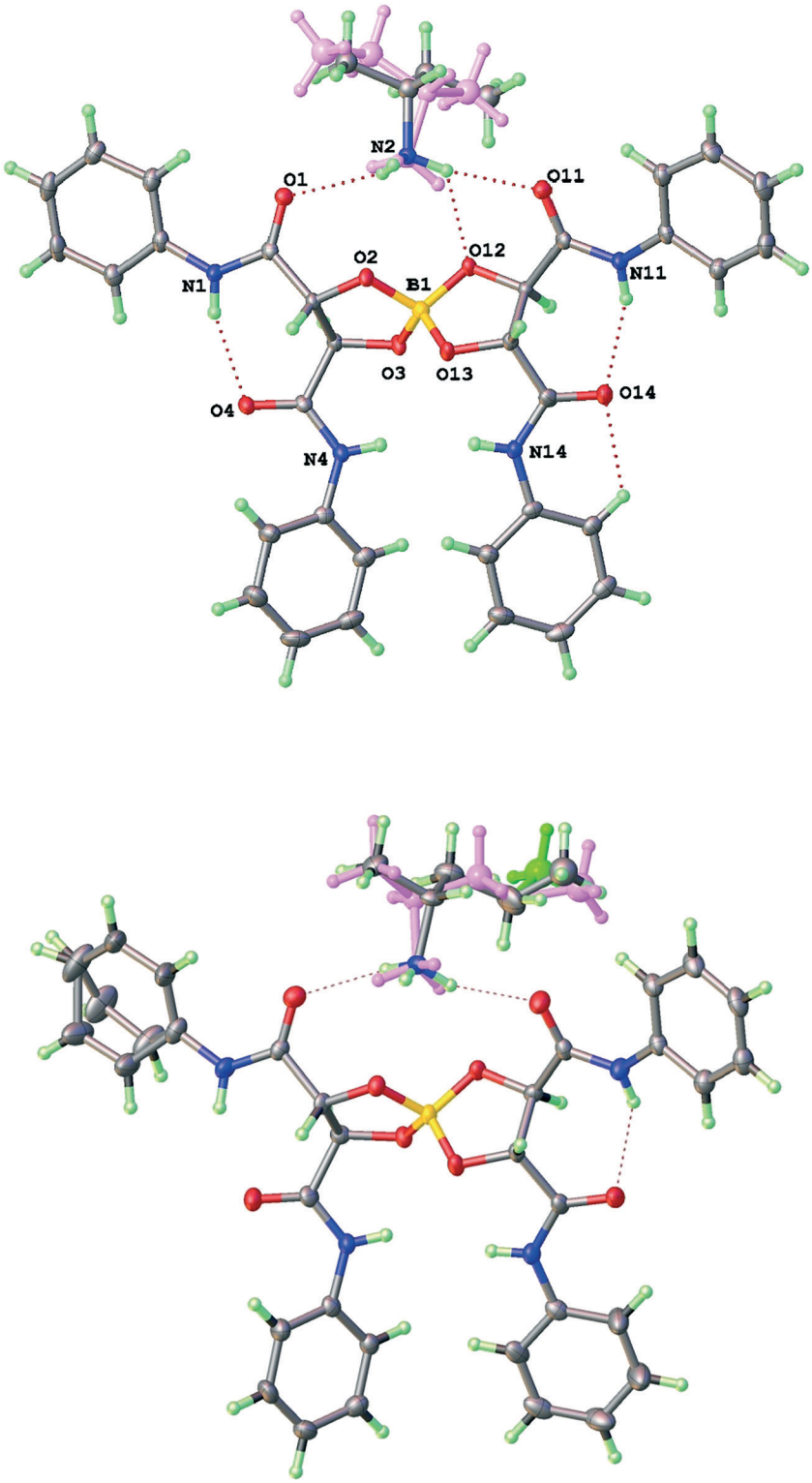

Fig. 5 a) Ion pair in [R/(S)-NH_3CHMeEt][B{L-Tar(NHPh)$_2$}$_2$] **5**, with disordered cation due to Me/Et exchange. b) Ion pair [R/(S)-NH_3CHMePr][B{L-Tar(NHPh)$_2$}$_2$] **6**, with CH pyramidal disorder. The minor S-components are shown in pink.

manner to 5 and the solid was isolated in reasonable yield and phase purity. This time the space group was monoclinic $P2_1$, although some conserved packing features are seen. A molecular ion pair is shown in Fig. 5b and reveals that once again a solid solution is formed which limits enantiopurity, but this time the location of –Me, –^{n}Pr and –NH_3 substituents at the chiral centre remain roughly in place, whilst there is a 'pyramidal' disorder of the C–H group (Fig. 9b). The chiral

carbon itself thus has two alternate orientations and can be refined to approximately 61 : 39 ratio.

This disorder mode is possible for many chiral molecules possessing a simple –H substituent at the chiral carbon. Indeed, the larger or more highly functional the three other substituents, the more prevalent it can become, since preserving their relative packing arrangement would be increasingly important. Once again given the relatively poor direct resolution further recrystallizations to enhance the enantiopurity of salt **6** were not attempted.

It was however encouraging to note that various structural features of **6** were preserved from **5**. The spiroborate anion had a similar overall geometry, with Y-shape conformation, intra-molecular amide H-bonds and an organoammonium 'binding pocket' with two NH---O=C H-bonds within an ion pair and the third NH hydrogen bonding to an anion translated along a short 5.5 Å axis, which again was the crystallographic [100] direction. Hence both in both structures in-register layered stacking is found along the common short axis.

A further perturbation of the amine structure was then made by replacing the aliphatic Et or ^{n}Pr groups with a Ph substituent. Once again a 1-pot solvothermal crystallization in methanol–water was carried out to effect a possible resolution of the racemic amine. This time the resulting crystalline solid produced the product phase [R-NH_3CHMePh][B{L-Tar(NHPh)$_2$}$_2$] **7** which belongs to the monoclinic system with space group $P2_1$. Like the Na salt **4** it is solvated, with one methanol disrupting the amide hydrogen bonding. The asymmetric unit contains one formula shown in Fig. 6a. A specimen of **7** gave 88 : 12 ratio of R- to S- within the crystal. A difference electron density map gave peaks of 3.26 and 0.56 eÅ^{-3} respectively for the major and minor components of the –CH_3 group, shown in Fig. 7. The lower level of disorder/solid solution in **7**, compared to the *sec*-butylammonium analog **5**, can be traced to the different chiral environment found around the cation, as shown in Fig. 10 as viewed along the short *a*-axis. Each cation is surrounded by five neighbors in the bc plane. One is the [B{L-Tar(NHPh)$_2$}$_2$]$^-$ anion to which the –NH_3 head forms two hydrogen bonds, two other [B{L-Tar(NHPh)$_2$}$_2$]$^-$ make weak aryl-H contacts and the other two neighbors are other cations, which form the 2_1-screw arrangement along the *b*-axis.

It should be noted that the ghost peak for the Me of the S-cation does not lie along the C–H vector for the R-cation, but is rotated so that C–H---O interaction is still maintained. The ellipsoid of the chiral carbon is clearly elongated indicating it should have a split position, although the geometry of the NH_3 and Ph groups are not greatly perturbed. The description of the disorder as H/Me exchange is hence a best approximation and may be seen as a starting point from which the minor component makes a best fit to the surrounding structure.

Recovery of α-methylbenzylamine from the salt **7** and derivatization of the amine group to form the benzamide PhCONHCHMePh allowed for chiral HPLC chromatography which confirmed (Fig. 8) the 88-R : 12-S ratio in excellent agreement with the X-ray structure from an individual crystal. This 76% ee for a first crystallization step is still very respectable. A single re-crystallization of this material from pure methanol (80% yield) afforded a crystal **7b** with no observable peaks for the minor *S*-enantiomer. The largest other residual peak in the original crystal of **7** of *ca.* 0.3 eÅ^{-3} that lay in the vicinity of the non-coordinated methanol also disappeared, supporting the idea that this was in fact due to a small component of water which was inserted into the amide hydrogen bond instead of methanol, when the crystallizing solvent was a 3 : 1 methanol : water mixture.

Whilst the R- and S-cations are not perfectly discriminated in **7** the potential of [B{L-Tar(NHPh)$_2$}$_2$]$^-$ or related bora–tartramide anions for chiral resolution is well demonstrated. The reasonable success with the resolution of **7**, but with the –H/–Me disorder at the chiral centre led us to next investigate the resolution of the ethyl analogue, for which such disorder should be reduced or eliminated. Accordingly a similar 1-pot resolution was attempted using *rac*-1-phenylpropylamine and the structure of the resulting salt [S-NH_3CHEtPh][B{L-Tar (NHPh)$_2$}$_2$]·MeOH **8** was determined and consistent with effective resolution in a single step. The compound was not isostructural with **7**, but crystallizes in space group *C*2. This time a short 5.4 Å repeat due to stacking of molecular layers was found for the monoclinic *b*-axis. The asymmetric unit and ion pair are shown in Fig. S2.† The disposition of Ph and Et substituents is reversed compared to **7** so that the predominant enantiomer is now S-, rather than R-. No discernable peaks for pyramidal or other disorder could be found and chiral HPLC confirmed the cations in the isolated solid were close to pure *S*-enantiomer.

The prevalence of three different disorder modes in the four racemic amine systems tested indicated the inherent difficulties in the diastereomeric salt resolution method for such amines with high levels of molecular similarity for their enantiomers. Our previous success with [BMan$_2$]$^-$ also included one example 1,2-diaminopropane with extremely similar enantiomeric cations. Given the partial success of the boron tartramide [B{L-Tar(NHPh)$_2$}$_2$]$^-$ in the resolution of α-methylbenzylamine, we decided to make one further change by replacing the –Me group with –CH_2OH. It was anticipated that the introduction of an addiional hydrogen bonding group to augment the –NH_3 might also lead to superior discrimination between enantiomers. Accordingly the 1-pot reaction of *rac*-2-phenylglycinol was attempted which afforded [S-NH_3CH(CH_2OH)Ph][B{L-Tar-(NHPh)$_2$}$_2$]·MeOH, **9**.

Interestingly the powder XRD pattern of **9** indicated a striking similarity to that of **7** and single crystal structure analysis confirmed the isomorphic nature of the two phases. In **9** however the hydroxymethyl –CH_2OH group appears close to fully ordered in replacing the disordered –Me.

The arrangement shown for the ion-pair of the asymmetric unit in Fig. 6b is essentially identical to that for **7**. The work

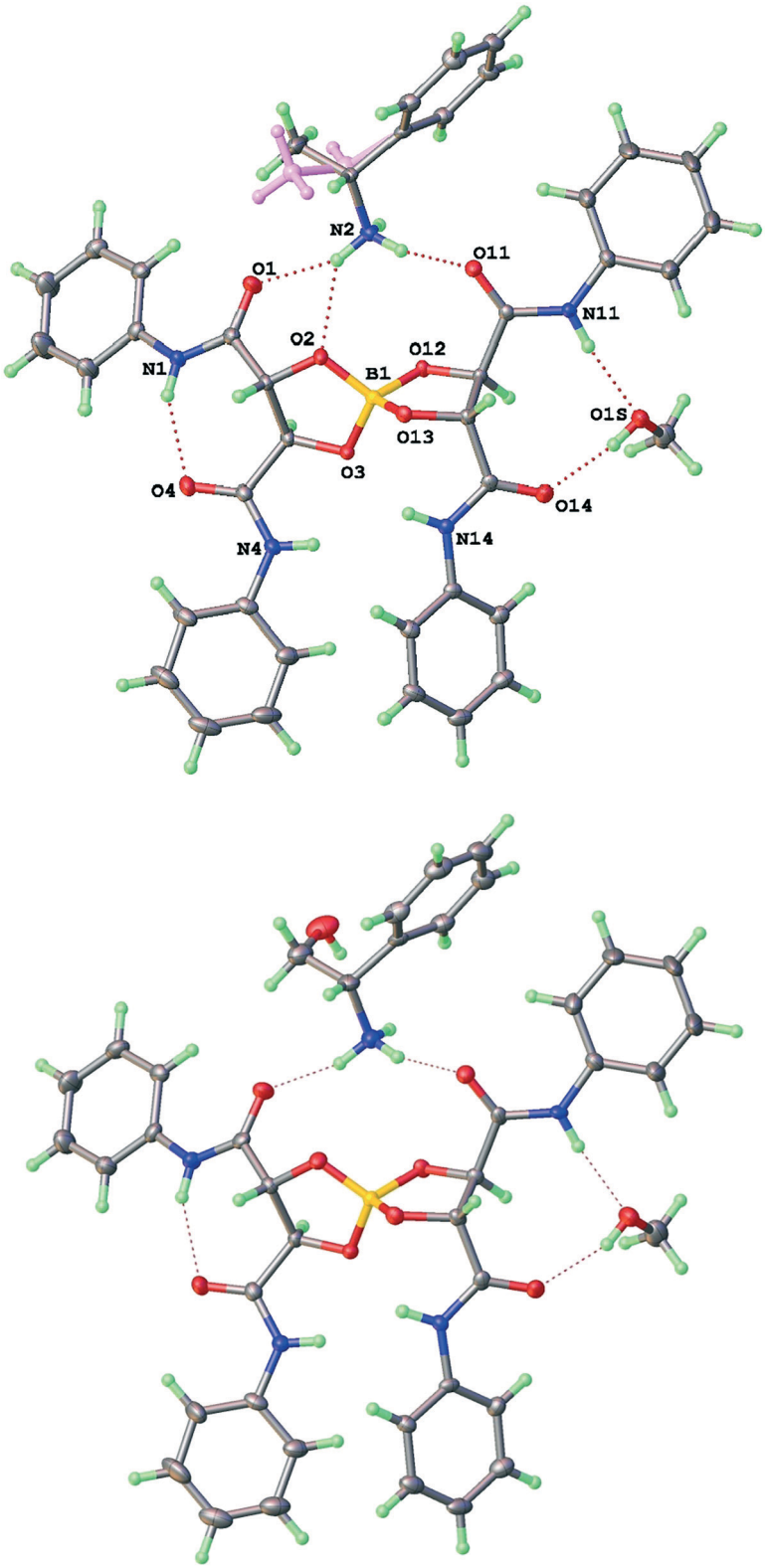

Fig. 6 a) Structure of ion pair in **7** [R-$NH_3CHMePh$][B{L-Tar$(NHPh)_2$}$_2$]·MeOH, and b) the isostructural **9** [S-$NH_3CH(CH_2OH)Ph$] [B{L-Tar$(NHPh)_2$}$_2$] ·MeOH.

up of the isolated solids from **9** gave chiral HPLC with 94% ee. The X-ray structure of **9** has very weak ghost peaks at the cation sites which in view of the chiral HPLC result can be seen as a 97S : 3R disorder. This indicates the practical limit for X-ray identification of the diastereomeric solid-solutions is around 95% ee.

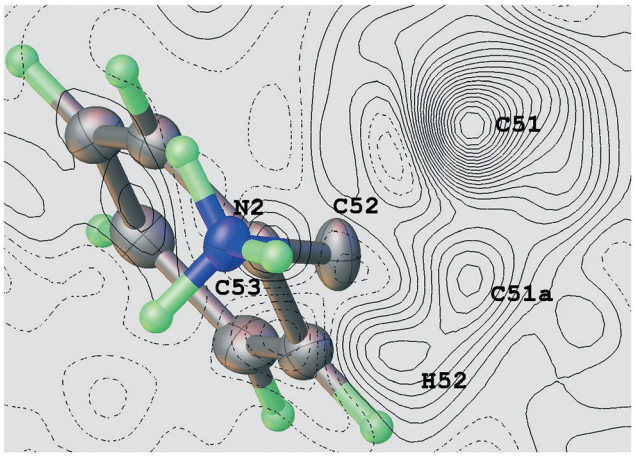

Fig. 7 Difference electron density map of disordered cation in **7**. Showing minor-CH_3 position C(51a) lying between major-CH_3 C(51) and major-H H(52).

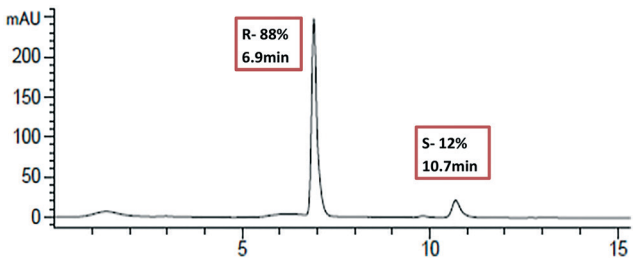

Fig. 8 Chiral HPLC chromatogram of PhCONHCHMePh enantiomers derived from **7**.

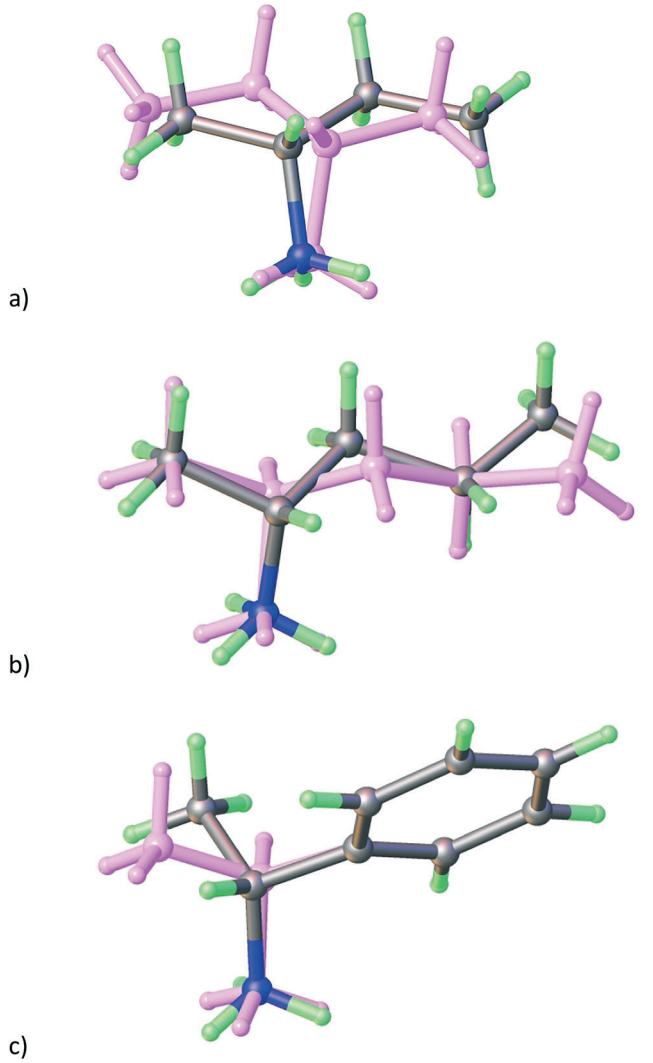

Fig. 9 Cation disorders in a) [NH_3CHMeEt] in **5**, b) [NH_3CHMePr] in **6** and c) [NH_3CHMePh] in **7**.

Cation disorder modes and environments

The disorder of the cations in salts 5–7 can be considered first in terms of the three possible modes of disorder presented earlier, namely H/R_1 exchange, R_1/R_2 exchange and CH re-pyramidalization. These were considered and computed in the model chiral system CHFClBr as ways of comparing shape similarity based on overlap of molecular wavefunctions.[29] The overlay of major and minor cation components in 5–7 are shown in Fig. 9.

In **5** the *sec*-butyl-ammonium ion has a minor component (34%) in which the Me and Et group positions are clearly reversed – an R_1/R_2 site exchange. This is accompanied by a slight splitting of the ammonium N position (0.20 Å) and a change of the N–C bond vector (19°). This leads to a more pronounced splitting of the chiral carbon position (0.52 Å) and exchange of the Me and Et group positions, such that the Me carbon in each orientation is just 0.54 Å from the terminal C of the Et groups of the other hand. The two components thus form an almost perfect mirror image with each other.

In **6** [NH3CHMePr] the extension of Et to Pr changes the disorder mode in order to fit to the cation environment to a C–H re-pyramidalization for the minor 36% component. In this the NH_3 and Me retain common sites but the chiral C position is split by 0.78 Å and the C–H are oriented away from each other (2.73 Å). The n-propyl arms comprise overlapped zig-zag chains that share a common site for the central CH_2 group. The terminal CH_3 of the propyl chain of the major component is also split, which is apparently linked to orientational disorder of a Ph ring in a neighboring anion.

In the [NH_3CHMePh] salt **7** the NH_3 and Ph retain common sites, whilst the Me position is clearly split (1.48 Å). Modelling indicates there should be a slight spitting of the chiral center by 0.29 Å and the vectors for the major and minor C–H directed about 145° apart. This disorder is best described as a hybrid of C–H/Me disorder and CH repyramidalization. Pure CH/Me disorder would have common H/Me vectors for major/minor components and pure repyramidalization a common Me position for both hands.

In the case of salt **9** the [S-NH_3CH(CH_2OH)Ph] cation occupies a similar crystal site to that in the isomorphous **7**,

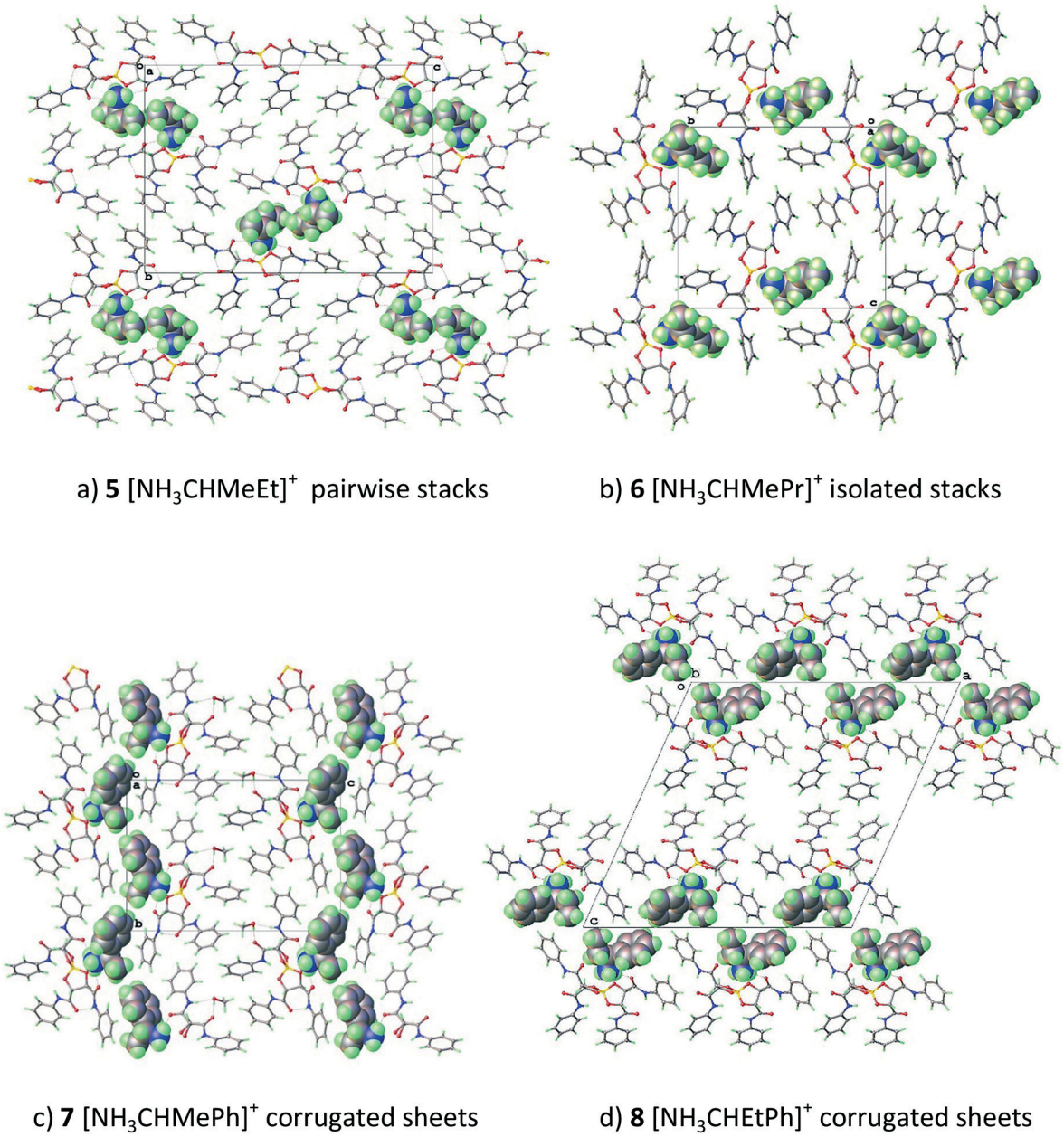

Fig. 10 Cation environments and self-associations in **5**–**8**, (a–d respectively) all viewed along short 5.5 Å axis.

however the conversion of CH_3 to CH_2OH forms an additional H-bond that helps lock in the major component. It should be noted that switch to S-configuration in **9** from R in the major component of **7** is due to the higher priority of CH_2OH compared the Ph in the Cahn–Ingold–Prelog priority rules.

Whilst the origin of the preference in the case of **9** may be clearly traced, this is harder for cases **5**–**7**, for which the dual orientations of R- and S- are required to be similar in energy. All structures have similar short 5.5 axis repeats that derive from the NH_3 binding and roughly planar anion shape. The 'tetradentate' binding pockets use two N–H in binding to the anion and the other one to the next anion along the 5.5 Å stack. The packing environments of the cations may be examined by viewing along the 5.5 Å axis, *i.e.* along (100) direction for **5**–**7** and (010) for **8**.

The arrangements and metrics in these projections show unique packing and cation environments in each case. In **5** a pocket with two cations surrounded by parts of four different anions is found. The cations make no strong interactions that would clearly orient the Me and Et groups, but the pairwise arrangement may facilitate Me/Et orientational disorder. In **6** the cations form isolated stacks along the 5.5 Å axis, which are surrounded by parts of three anions. The Pr group position is clearly differentiated from the Me, but the disorder is now CH re-pyramidaliztion. This has chiral

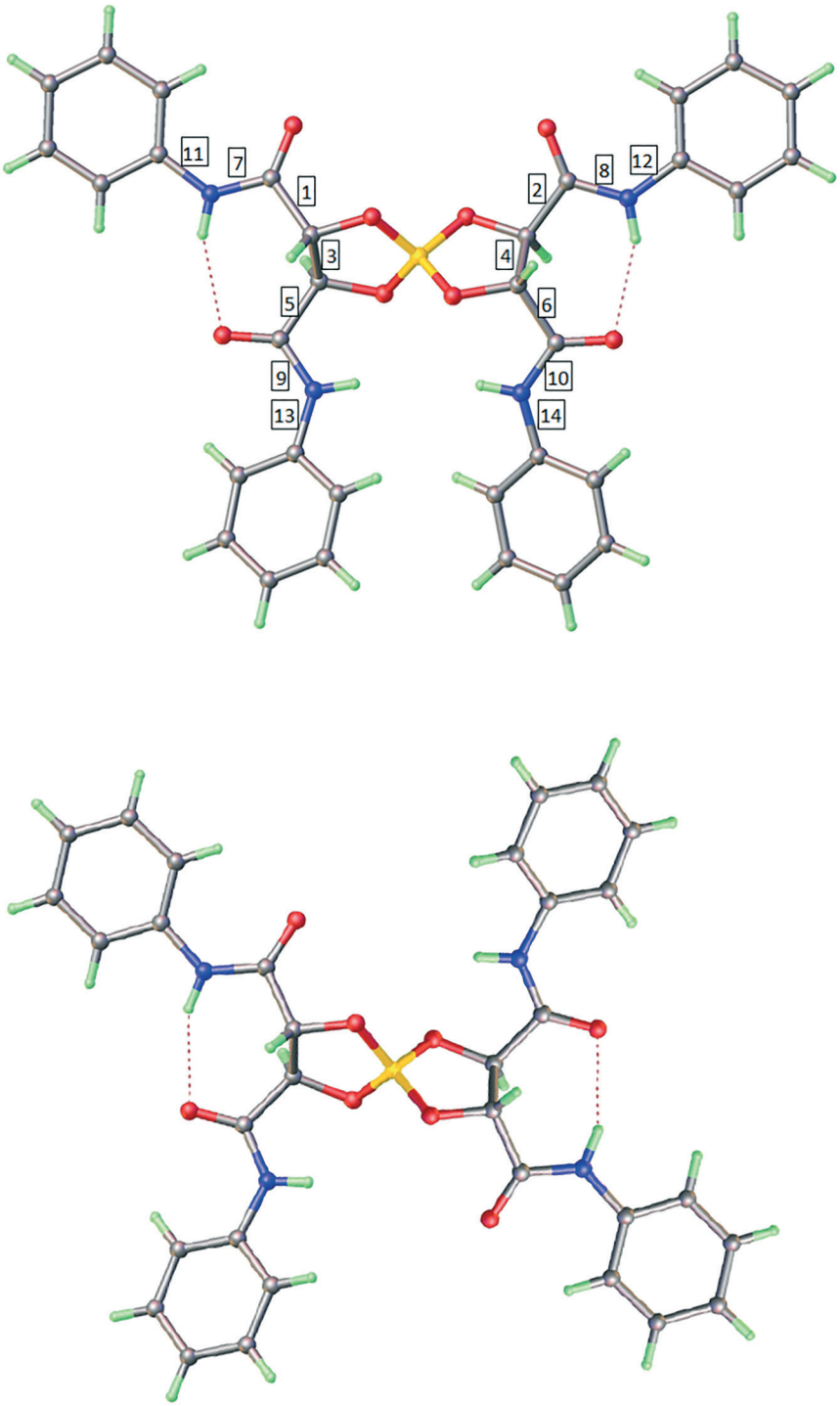

Fig. 11 "Y-shape" $[B_S\{L\text{-}Tar(NHPh)_2\}_2]$ anion – labelling scheme refers to torsion angles in Table 2 and hypothetical "X-shape" conformation for the $[B_R\{L\text{-}Tar(NHPh)_2\}_2]^-$ anion.

carbon CH oriented closer to a keto O (H---O 2.94 Å) for the major R-component, which may help explain its preference for incorporation in the structure.

In **7** the cations form a corrugated sheet, which have closer contacts between CH_3 and Ph of neighboring cations for the major R-component. Each cation is contacted by parts of just three anions. In the [S-NH_3CHEtPh] salt **8** the cations may also be considered to form corrugated sheets, but in this case Et---Et and Ph---Ph make ordered close contacts.

Geometry of $[B\{L\text{-}Tar(NHPh)_2\}_2]^-$ spiroborate anions

The bis(*N*,*N*′-diphenyltartramido)borate ions are readily prepared from L-tartaric acid in two facile steps. Since a similar

synthesis can be extended to using many aromatic amines in the place of aniline the $[B\{L\text{-}Tar(NHPh)_2\}_2]^-$ anion can be viewed as the parent in a large family of chiral aromatic spiroborates derived from aryltartramide ligands. These might have considerable potential for resolution, so what features supporting this idea can be gained from these studies of $[B\{L\text{-}Tar(NHPh)_2\}_2]^-$ salts **2–9**?

Firstly, all salts are quite crystalline and apart from the issues associated with R/S-cation disorder most structures show well-ordered arrangements with quite strongly defined conformational preferences. The geometric features of $[B\{L\text{-}Tar(NHPh)_2\}_2]^-$ anions in selected salts are summarized for comparison in Table 2 with torsion angles labeled as in Fig. 11.

Since all structures are well determined at low temperature of 100 K, even the B–O bond lengths are to reasonable precision of 0.002–3 Å. The range found in the *sec*-butylammonium salt **5** of 1.450–1.485(3)Å encompasses the narrower range of values found in the other salts too. Since all four arms of the anion are in principle chemically identical this is anticipated, some variation is introduced primarily due to coordination to K, Na or N–H hydrogen bonding to the B–O oxygen atoms. The B–O bond lengths in these diolates are intermediate to the B–O of 1.43–1.45 Å for phenoxy and 1.49–1.51 Å for carboxy groups in bis(mandelato)borate, $[BMan_2]$ anions.[6] An even wider disparity of B–O lengths of 1.345 to 1.525(7)Å was found in an open-framework vanadoborate possessing both 3- and 4-coordinate borate centres.[30]

The five membered spiroborate rings are roughly planar but all exhibit slight puckering. This in line with the situation for the 5-membered ring chelate rings in $[BMan_2]^-$,[5] but contrasts with strongly puckered 6-membered rings found in bis(salicylato)borate $[B(Sal)_2]^-$.[31] The root-mean square displacements are less than 0.1 Å. In general the C and O atoms tend to be more displaced than the boron. The *syn* O–C–C–O torsion of -56° found in the parent diol **1** is thus reduced to less than 10° for the diolate torsion angles (**3** and **4**) in the unsolvated anions, though the methanolated structures have an increase to about 28° on the solvated side. The tartramido ligand O–B–O 'bite angles' lie in a narrow range bound by the value of 104.2 and 105.6° found in **4**. These bite angles are close enough to ideal tetrahedral values to induce little angular strain and help explain why the five membered rings (which require 108° angles on average) are close to planar.

Ligand asymmetry has already been described as resulting from the tendency to form intra-ligand NH---O=C H-bonds between two amide groups within each ligand. This is the case for **2**, **3**, **5** and **6**, whilst in **4**, **7**, **8** and **9** the arrangement is just slightly modified by inserting a MeOH solvent (or water) molecule into the hydrogen bond arrangement. This maintains the asymmetry whilst introducing a perturbation to the preferred geometry of the anion. The overlay of anion geometries for the K and Na salts was shown in Fig. 3, in fact as Table 2 indicates, there is also fairly close preservation of geometry from the K salt **2** to the *sec*-butylammonium salt **5**, and a similar preservation from the solvated Na salt **4** to the methanol-solvated α-methylphenylammonium salt **7**.

The phenyl ring orientations at the top of the 'Y-shape' are reasonably close to co-planar with the amide (torsion angles 11 & 12) due to the reinforcing effect of C–H---O interactions. The phenyl rings at the stem or bottom of the 'Y-shape' are a little more variable in their orientation (torsions 13 & 14) with values from +20.0 to −29.0°. In short the bis(tartramido)borate anions have some fairly well defined conformational preferences, especially when cation binding through coordination or hydrogen bonding is involved, but with some built-in degrees of flexibility.

DFT calculations on $[B\{L\text{-}Tar(NHPh)_2\}_2]^-$

We have investigated the relative energetics of spiroborate anions and some ion pairs for the 'Y-shape' $[B_S\{L\text{-}Tar(NHPh)_2\}_2]^-$ and 'X-shape' $[B_R\{L\text{-}Tar(NHPh)_2\}_2]^-$ (Fig. 11) using DFT calculations[32] and the Gaussian09 package.[33] Since solvent effects on the related $[B(Man)_2]^-$ system indicated only minor perturbation in the relative energies from the gas phase to solution, this was not carried out for the $[B\{L\text{-}Tar(NHPh)_2\}_2]^-$ anions. Interestingly the isolated gas phase ions indicate that the individual 'X-shape' ions are notably more stable, (7.2 kcal mol^{-1}) however introduction of a chelating K^+ ion in an isolated ion-pair reverses the stability, once again with a considerable energetic difference (20.3 kcal mol^{-1}). Neither case is a fair indication of the situation found for either alkali metal or organoammonium salts in the solid state however, since in the crystal the anions interact with several counterions, rather than just one. However the 'tetradentate pocket' found in the solid state for the 'Y-shape' in coordination binding to metals, or for H-bonding to RNH_3^+ cations, is clearly a stabilizing feature that can explain the exclusive observation of this conformer in the structures of **2–9**, despite the supposed energetic favorability of the less polar 'X-shape'. As further salts of $[B\{L\text{-}Tar(NHPh)_2\}_2]^-$ are isolated, especially with non-coordinating counter cations, it may be anticipated that the 'X-shape' structure and other arrangements will eventually be encountered. In both X- and Y- cases the DFT calculations faithfully reproduce the pair of intramolecular NH–OC amide hydrogen bonds found in the unsolvated crystal structures **2** and **5**, which break the potential D_2 symmetry of the anions, by introducing ligand asymmetry. These will undoubtedly remain a feature, unless disrupted by the insertion of a H-bonding solvent, such as MeOH or H_2O as found in structures **4** and **7**. Tartramides without N–H functionalities, or tartrate esters would be expected to have greater scope for individual freedom of the substituent arms without the internal N–H---O=C hydrogen bonds, which may or may not be better for general crystallization purposes.

Whilst the exclusive solid state favoring of the 'Y-shape' in the salts studied here can be rationalized by the preferred coordination or H-bonding, in solution it is probable that no

major conformational preference is found, since the ^{1}H NMR indicates a singlet for the tartramide C(2)–H–C(3)–H protons, due to rapid equilibration between X- and Y- and other forms. Either X- or Y- alone should give two doublet signals due to coupling of inequivalent protons. However in solution they are rapidly interconverting through amide H-bond breaking, amide rotation and amide H-bond reformation. A mixed population of X-, Y- and other conformers in solution may assist resolution crystallizations in a similar manner that we have speculated may operate for $[BMan_2]^-$. Since one half of the molecular shape is retained whilst the other half is not, the presence of the X-conformer may disrupt nucleation to differing extents for the two diastereomeric Y-type salts. This is believed to be the basis for the 'Dutch method'[34] in which the presence of a related resolving ion may considerably improve the efficiency of a resolution, despite the fact it is not incorporated in the final solid.

Future prospects of chiral spiroborates

For diastereomeric salt formation, the development of new synthetic anions with high chiral discriminating power for resolution or catalysis is a desirable objective.[35] One notable system developed by Lacour involves the TRISPHAT anions $[P(O_2C_6Cl_4)_3]^-$ which are based on non-labile tris-chelation of substituted catecholates.[36] These have good efficiency in a variety of chiral resolutions, but remain relatively expensive, limiting their attractiveness and bulk industrial use. Other anions have also been proposed for use in recent times,[37] including some applied to similar amines to those described here.[38]

Chelation of boron by diols, acid-alcohols, catechols and salicylic acids can result in spiroborate anions which can have a variety of uses.[39] Some such as bis(catecholato)borate $[BCat_2]^-$, have been demonstrated to be effective crystallizing anions.[40] Their use in resolution was first reported by Periasamy who made an improved resolution of BINOL based on forming a diastereomeric salt of its borate ester.[41] This approach was then used in resolution or purification of other diols.[42] Conversely the use of chiral $[B(BINOL)_2]^-$ anions was then applied to resolution of chiral amines and amino-alcohols.[43] This established the effectiveness of such anions, but its use by others has been limited since the cost of resolved BINOL remains very high. Despite this promising work the use of spiroborates for resolution has not received much further attention, though effective chiral resolution using a chiral diborate has been demonstrated.[44] One factor is that the chiral borate centres are labile and prone to racemization. However we have recently demonstrated that B-chiral spiroborate anions from salicylate $[B(Sal)_2]$ can be successfully isolated in enantiopure forms and that they are stable in aprotic solution.[31]

Fogassy *et al.* have noted not only the intuitive result that diastereomeric salts with higher melting points will tend to precipitate in chiral resolutions, but also that solvates can be favored, whereas amorphous solids are strongly disfavored.[45] Regarding the resolution potential of spiroborate anions, a successful resolving agent must crystallize effectively with the organoammonium cation with sufficient overall difference in stability and hence solubility, between the potential diastereomeric salts formed. It should also minimize the likely contamination of a given phase with the cation of opposite chirality through disorder and solid-solution formation. As we have found for $[BMan_2]$ variation in solvent can have a profound impact, especially if solvates are formed, as for $[1,2\text{-dap-H}_2][BMan_2]\cdot MeOH$.[5] This clearly applies to the tartramide spiroborates since several methanolates have been found in the chiral resolution systems studied herein, screening of many solvents may provide superior resolutions to those we present here, which are not meant to represent optimal resolutions using these anions, but establish their generic potential as resolving agents.

The promising results for resolution from both our earlier studies[5] on bis(mandelato)borate $[BMan_2]^-$ and the new findings for $[B\{L\text{-Tar(NHPh)}_2\}_2]^-$ anions presented here are encouraging. The relatively facile preparation of the chiral tartramide diol **1** using aniline can be readily extended to other aromatic amines. The resulting aryltartramides will provide a family of related chiral spiroborate anions. It may be reasonably expected that chiral resolutions, such as those presented here, may then be more fully explored and optimized, since both CH–pi interactions[46] and the influence of substituent groups[47] on resolutions are both well established.

Experimental

Synthesis and characterization

All chemicals were reagent grade (99%+) (Sigma-Aldrich, TCI or Acros). Elemental combustion analyses were carried out by Medac Ltd., Surrey, U.K.

***N*,*N*′-Diphenyl-L-tartramide [L-Tar(NHPh)$_2$-H$_2$] (1).** The synthesis of 1 followed an adaptation of the published procedure of Chen *et al.*[48] L-Tartaric acid was directly amidated by refluxing in a two stage approach i) a mixture of xylenes (25 mL) aniline ($C_6H_5NH_2$ Mw 93.1, d = 1.02 g mL^{-1}, 5.0 mL, 55 mmol) and L-tartaric acid ($C_4H_6O_6$, Mw 150.1, 2.25 g, 15.0 mmol) were refluxed for 2 h. ii) 2.5 mL dimethylformamide (DMF) was then added and the mixture refluxed for a further 3 h. Upon cooling a white solid (1) was formed which was filtered and washed with water and then 95% EtOH to yield crystalline (1) as colorless transparent plates ($C_{16}H_{16}N_2O_4$, Mw 300.3, 4.05 g, 13.5 mmol, 90% yield). CHN: found (calc.) %C = 64.17 (63.99); %H = 5.31 (5.37); %N = 9.41 (9.33).

K[B{L-Tar(NHPh)$_2$}$_2$] (2). The potassium salt K[B{L-Tar(NHPh)$_2$}$_2$] 2 of the spiroborate anion derived from chiral diol [L-Tar(NHPh)$_2$-H$_2$] 1 was synthesized by a 1-pot solvothermal reaction/crystallization approach. 300 mg (1 mmol) of [L-Tar(NHPh)$_2$-H$_2$], 31 mg (0.5 mmol) of boric acid and 28 mg (0.5 mmol) of KOH were heated in 0.6 mL MeOH at 110 °C for 1d. Colorless block crystals were filtered and washed by minimal amount of water and acetone affording

284 mg of 2 ($C_{32}H_{28}BKN_4O_8$, Mw = 646.5, 88% yield). CHN: found (calc.) %C = 58.98 (59.45); %H = 4.65 (4.37); %N = 8.52 (8.67). A single crystal specimen for X-ray structure analysis of **2**, was selected directly from the solvothermally crystallized solid.

NH_4[B{L-Tar(NHPh)$_2$}$_2$] (3). 300 mg (1 mmol) of [L-Tar(NHPh)$_2$-H_2], 31 mg (0.5 mmol) of boric acid and 40 μL (0.6 mmol) of 30% aq. NH_4OH were heated in 0.6 mL MeOH at 110 °C for 1d. Colorless needle crystals were filtered and washed by minimal amount of water and acetone affording 256 mg of 3 ($C_{32}H_{32}BN_5O_8$, Mw = 625.4, 82% yield). CHN: found (calc.) %C = 61.39 (61.45); %H = 5.14 (5.16); %N = 11.03 (11.20).

Na[B{L-Tar(NHPh)$_2$}$_2$]·2MeOH (4). 300 mg (1 mmol) of [L-Tar(NHPh)$_2$-H_2], 31 mg (0.5 mmol) of boric acid and 20 mg (0.5 mmol) of NaOH in 1 mL MeOH were heated solvothermally at 80 °C for 2d. Colorless crystal platelets were filtered and washed by minimal amount of water and acetone affording 257 mg of **4**, which was a di-methanol solvate ($C_{32}H_{28}BN_4NaO_8$, Mw = 694.4, 74% yield). CHN found (calc. best fit for 4 with 1.5MeOH) %C = 58.66 (59.48), %H = 4.62 (4.77); %N = 8.78 (8.28).

[R/(S)-NH_3CHMeEt][B{L-Tar(NHPh)$_2$}$_2$] (5). 300 mg (1 mmol) of [L-Tar(NHPh)$_2$-H_2], 31 mg (0.5 mmol) of boric acid and 75 mg (1 mmol) of *rac-sec*-butylamine (NH_2-CHMeEt) were heated in 1 mL of a 3:1 MeOH:H_2O mixture at 110 °C for 1d. 273 mg of **5** were isolated as colorless crystal plates ($C_{36}H_{40}BN_5O_8$, Mw = 681.6, 80% yield). CHN found (calc.) %C = 63.42 (63.44); %H = 5.84 (5.92); %N = 10.25 (10.28).

[R/(S)-NH_3CHMePr][B{L-Tar(NHPh)$_2$}$_2$] (6). 300 mg (1 mmol) of [L-Tar(NHPh)$_2$-H_2], 31 mg (0.5 mmol) of boric acid and 90 mg (1 mmol) of *rac*-2-pentylamine (NH_2CHMePr) were heated in 1 mL MeOH at 110 °C for 2d. 288 mg of unsolvated **6** were isolated as colorless needles ($C_{37}H_{42}BN_5O_8$, Mw = 695.6, 82% yield).

[R/(S)-NH_3CHMePh][B{L-Tar(NHPh)$_2$}$_2$]·MeOH (7). 300 mg (1 mmol) of [L-Tar(NHPh)$_2$-H_2], 31 mg (0.5 mmol) of boric acid and 118 mg (1 mmol) of *rac*-1-phenylethylamine(NH_2-CHMePh Mw = 121.2, d = 0.94 g mL^{-1}, 0.125 mL) were heated in 1 mL MeOH at 110 °C for 5d.; 324 mg colorless platy crystals of **7** isolated as a MeOH solvate ($C_{40}H_{40}BN_5O_8.CH_4O$ Mw = 761.6, 85% yield). CHN found (calc. For 7 with 1.0MeOH) %C = 63.96 (64.66), %H =5.14 (5.82), %N = 9.17 (9.20). A single crystal XRD and chiral HPLC were also run on a sample (**7b**) obtained by recrystallization (80% yield) of product **7** from pure MeOH and these compared well with the compound directly obtained from commercial R-α-methylbenzylamine (99% ee).

[S-NH_3CHEtPh][B{L-Tar(NHPh)$_2$}$_2$]·MeOH (8). 300 mg (1 mmol) of [L-Tar(NHPh)$_2$-H_2], 31 mg (0.5 mmol) of boric acid and 135 mg (1 mmol) of *rac*-1-phenylpropylamine(NH_2CHEtPh Mw = 135.2, d = 0.94 g mL^{-1}, 0.145 mL) were heated in 1 mL MeOH at 110 °C for 2d.; 326 mg colorless needle crystals of **8** isolated as a mixed MeOH/H_2O solvate ($C_{41}H_{42}BN_5O_8.0.25CH_4O{\cdot}H_2O$, Mw = 767.1, 85% yield).

[S-NH_3CH(CH_2OH)Ph][B{L-Tar(NHPh)$_2$}$_2$]MeOH (9). 300 mg (1 mmol) of [L-Tar(NHPh)$_2$-H_2], 31 mg (0.5 mmol) of boric acid and 140 mg (1 mmol) of solid *rac*-2-phenylglycinol (NH_2CH(CH_2OH)Ph, Mw = 137.2) were heated in 1 mL MeOH at 110 °C for 2d.; colorless needles were filtered and washed affording 305 mg of **9** as MeOH solvate ($C_{40}H_{40}BN_5O_9.CH_4O$ Mw = 777.6, 78% yield). CHN: found (calc.) %C = 63.0 (63.33); %H = 5.44 (5.70); %N = 9.23 (9.01).

X-Ray structure determinations

The X-ray structures of compounds **2–9** were determined after suitable single crystal specimens were grown, either directly through solvothermal synthesis, or by recrystallization as described in the synthesis section. All specimens are reasonably stable and the methanolates do not desolvate rapidly at ambient temperature, though they were handled quickly before transferring to the cold stream. The specimens were fixed in a cryoloop using Paratone™ and diffraction intensity data were collected at low temperature (100 K) on a Rigaku-Oxford Diffraction Supernova diffractometer operating with a copper micro-focus source. The structures were solved (SHELXS) and refined (SHELXL) using SHELX software[49] embedded in the Olex2 software platform,[50] which was also used to generate the molecular figures and graphics. The key structural parameters are given in Table 1, with fuller crystallographic details in the ESI.† All non-hydrogen atoms were refined with anisotropically excepting those of minor components which were isotropic and with bond length restraints applied. Protonation states of alkaloid cations were clearly established by identification of sensibly located electron density peaks for H associated with N heteroatoms on ammonium and amide centres. Where practicable these were refined isotropically, or for disordered cases, these were placed and treated with geometric riding constraints (d_{N-H} = 0.88 Å) as were all C–H hydrogen atoms. For the disordered cations the separate parts were refined with group occupancy factors that summed to unity and then fixed in the final refinement. In general, the values from S-XRD were in good agreement with values later obtained from chiral HPLC. In the case of **8** a solvent channel was identified with no well-defined peaks and the Squeeze functionality (Platon[51]) was applied.

Powder X-ray diffraction

The phase purity of products was established after X-ray structure determination by recording diffractograms (2θ = 5–40°) on PanAlytical Aeris, Empyrean or X'Pert powder diffractometers. These were then compared to simulated powder XRD profiles from the Mercury software package[52] and in some cases unit cells were derived from the fitting of d-spacings of experimental pXRD peaks by the programs TREOR[53] or DICVOL.[54] Generally experimental P-XRD were in good agreement with the patterns simulated from single crystal structure determinations (see ESI†) consistent with single phase products.

Table 1 Structure determination summaries for [B{Tar(NHPh)$_2$}$_2$] salts **2**–**9**

Compound	2	3	4	5
Formula	K [B{Tar(NHPh)$_2$}$_2$]	NH_4 [B{Tar(NHPh)$_2$}$_2$]	Na [B{Tar(NHPh)$_2$}$_2$] 2MeOH	[R/(S)-NH_3CHMeEt][B{Tar(NHPh)$_2$}$_2$]
Code name	Gem81a	Gem57d	Gem84	Gem71a
CSD number	145865	1844600	145866	145867
Empirical formula	$C_{32}H_{28}BKN_4O_8$	$C_{32}H_{32}BN_5O_8$	$C_{34}H_{36}BN_4NaO_{10}$	$C_{36}H_{40}BN_5O_8$
Formula weight	646.5	625.43	694.5	681.5
Temperature/K	100(2)	100(2)	100(2)	100(2)
Crystal system	Monoclinic	Monoclinic	Orthorhombic	Orthorhombic
Space group	*C*2	*C*2	$P2_12_12_1$	$P2_12_12_1$
a/Å	30.9006(5)	30.9663(9)	7.6104(2)	5.4928(2)
b/Å	13.4265(2)	13.3119(4)	15.1976(3)	21.2421(5)
c/Å	6.99592 (11)	7.0955(3)	29.4158(5)	29.4393(7)
α/°	90	90	90	90
β/°	94.2992(14)	93.965(3)	90	90
γ/°	90	90	90	90
Volume/Å^3	2894.34(8)	2917.92(17)	3402.21(11)	3434.97(13)
Z, *Z*′	4, 1	4, 1	4, 1	4, 1
ρ_{calc} g cm^{-3}	1.484	1.424	1.356	1.318
Radiation, μ mm	Cu Kα, 2.137	Cu Kα, 0.855	Cu Kα, 0.940	Cu Kα, 0.769
F(000)	1344	1312	1456	1440
Crystal size per mm^3	0.05 × 0.03 × 0.02	0.10 × 0.05 × 0.03	0.20 × 0.05 × 0.05	0.5 × 0.01 × 0.01
2*Θ* maximum/°	136	135	136	136
Index ranges	$-37 \le h \le 36$, $-15 \le k \le 16$, $-7 \le l \le 8$	$-38 \le h \le 38$, $-16 \le k \le 16$, $-8 \le l \le 8$	$-7 \le h \le 9$, $-11 \le k \le 18$, $-35 \le l \le 34$	$-6 \le h \le 4$, $-23 \le k \le 25$, $-29 \le l \le 35$
Total reflections (%)	11 280 (98.3%)	8914 (100.0%)	9737 (98.1%)	9855 (98.3%)
Data quality	[R_{int} = 0.0203, R_{sig} = 0.0248]	[R_{int} = 0.044, R_{sig} = 0.0400]	[R_{int} = 0.0308, R_{sigma} = 0.0401]	[R_{int} = 0.0305, R_{sigma} = 0.0571]
Data/restr./params.	5070/1/417	8014/1/422	6079/0/477	6178/30/506
Goodness-of-fit F^2	1.027	1.043	1.017	1.006
Final *R* indexes [*I* > = 2*σ*(*I*)]	R_1 = 0.0336, wR_2 = 0.0873	R_1 = 0.0425, wR_2 = 0.1147	R_1 = 0.0328, wR_2 = 0.0784	R_1 = 0.0404, wR_2 = 0.0865
Final *R* indexes [all data]	R_1 = 0.0348, wR_2 = 0.0884	R_1 = 0.0485, wR_2 = 0.1170	R_1 = 0.0368, wR_2 = 0.0803	R_1 = 0.0535, wR_2 = 0.0906
Diff. peak/hole eÅ^{-3}	0.95/−0.22	0.23/−0.23	0.17/−0.17	0.22/−0.20
Flack parameter	0.015(4)	−0.09(16)	−0.04(5)	−0.05(14)

Compound	6	7	8	9
Formula	[R/(S)-NH_3CHMePr][B{Tar(NHPh)$_2$}$_2$]	[R/(S)-NH_3CHMePh][B{Tar(NHPh)$_2$}$_2$] MeOH	[S-NH_3CHEtPh][B{Tar(NHPh)$_2$}$_2$] MeOH	[S-NH_3CH(CH_2OH)Ph][B{Tar(NHPh)$_2$}$_2$] MeOH
Code name	Lawr435	Gem64b	Lawr437	Lawr434
CSD number	1844601	145868	1844602	1844603
Empirical formula	$C_{37}H_{40}BN_5O_8$	$C_{41}H_{44}BN_5O_9$	$C_{42}H_{46}BN_5O_9$	$C_{41}H_{44}BN_5O_{10}$
Formula weight	695.56	761.72	775.67	777.62
Temperature/K	100(2)	100(2)	100(2)	100(2)
Crystal system	Monoclinic	Monoclinic	Monoclinic	Monoclinic
Space group	$P2_1$	$P2_1$	*C*2	$P2_1$
a/Å	5.56240(9)	5.52108(7)	28.6200(11)	5.51895(7)
b/Å	19.1848(3)	15.5073(2)	5.25819(14)	15.5145(2)
c/Å	16.7363(3)	22.1422(3)	28.6090(9)	22.2271(3)
α/°	90	90	90	90.00
β/°	95.1248(15)	94.8402(12)	113.834(4)	94.4499(12)
γ/°	90	90	90	90.00
Volume/Å^3	1778.85(5)	1888.99(4)	3938.2(3)	1897.44(4)
Z, *Z*′	2, 1	2, 1	4, 1	2, 1
ρ_{calc} g cm^{-3}	1.299	1.339	1.308	1.361
Radiation, μ mm	Cu Kα, 0.752	Cu Kα, 0.779	Cu Kα, 0.770	Cu Kα, 0.808
F(000)	736.0	804	1640.0	820.0
Crystal size per mm^3	2 × 0.05 × 0.05	0.30 × 0.08 × 0.05	0.15 × 0.05 × 0.03	0.10 × 0.07 × 0.05
2*Θ* maximum/°	136	136	136	136
Index ranges	$-6 \le h \le 6$, $-22 \le k \le 22$, $-16 \le l \le 20$	$-5 \le h \le 6$, $-18 \le k \le 18$, $-26 \le l \le 19$	$-34 \le h \le 32$, $-6 \le k \le 6$, $-22 \le l \le 34$	$-3 \le h \le 6$, $-18 \le k \le 18$, $-25 \le l \le 26$
Total reflections (%)	10 205 (98.1%)	10 786 (98.7%)	10 916 (99.4%)	10 612 (97.9%)
Data quality	[R_{int} = 0.0245, R_{sigma} = 0.0417]	[R_{int} = 0.0159, R_{sigma} = 0.0261]	[R_{int} = 0.0238, R_{sigma} = 0.0371]	[R_{int} = 0.0292, R_{sigma} = 0.0444]
Data/restr./params.	6296/7/569	6743/2/545	7008/2/564	6701/1/518

Table 1 *(continued)*

Goodness-of-fit F^2	1.011	1.010	1.039	1.042
Final R indexes $[I > = 2\sigma(I)]$	R_1 = 0.0300, wR_2 = 0.0702	R_1 = 0.0281, wR_2 = 0.0711	R_1 = 0.0364, wR_2 = 0.0950	R_1 = 0.0409, wR_2 = 0.1026
Final R indexes [all data]	R_1 = 0.0322, wR_2 = 0.0714	R_1 = 0.0291, wR_2 = 0.0719	R_1 = 0.0396, wR_2 = 0.0971	R_1 = 0.0434, wR_2 = 0.1045
Diff. peak/hole eÅ^{-3}	0.15/−0.18	0.35/−0.17	0.22/−0.16	0.34/−0.24
Flack parameter	0.10(8)	−0.17(6)	0.19(15)	0.08(15)

Table 2 Key structural parameters in selected $[B\{L\text{-}Tar(NHPh)_2\}_2]^-$ anions

	2 (K)	4 (Na)·2MeOH	5 (NH_3CHMeEt)	7 (NH_3CHMePh)·MeOH
B–O lengths	1.460–1.479(3)	1.466–1.478(2)	1.450–1.485(3)	1.467–1.474(2)
5MR d(Åx100)	−4, 0, 4, −6, 6: **5**	−4, −5, 11, −14, 12: **10**	−7, 9, −7, 2, 3: **6**	5, 3, −9, 12, −11: **9**
B–O–C–C–O: rms	4, 0, −4, 7, −7: **5**	−3, −7, 14, −17, 13: **12**	−7, 9, −7, 3, 2: **6**	9, −1, −6, 12, −14: **10**
Tors OCCO 1/2	9.3/10.0	23.4/−28.2	8.6/9.5	19.0/−17.0
Tors OCCO 3/4	6.2/9.3	7.7/27.1	5.5/7.0	3.5/28.1
Tors OCCO 5/6	−175.7/173.6	157.9/−179.0	174.8/172.2	166.3/176.6
Tors OCNC 7/8	−7.1/−8.8	8.3/−0.1	−5.7/5.1	3.6/−6.1
Tors OCNC 9/10	9.6/−3.1	0.0/4.0	1.7/1.1	2.1/0.2
Tors CCNC 11/12	−3.3/9.8	−9.7/−8.7	−12.6/−5.8	−7.7/−10.0
Tors CCNC 13/14	20.4/−2.0	−21.2/−7.7	−29.0/−12.2	−19.3/−26.2
Chelate OBO	105.1/105.0	105.6/104.2	104.5/105.4	104.7/104.4
Jaw OBO	109.8, 110.0 (K)/111.5, 112.8	111.7 (Na)/112.7	110.9 NH/110.4	112.8 NH/111.5

Chiral HPLC

The 1-phenylethylamine free base were isolated from the salt 7 by a similar procedure to that published for organoammonium salts of $[BMan_2]$.[5] The salt was treated with aq. NaOH (25%) and extracted (3×) into chloroform. The combined extracts were evaporated and recrystallized with methanol affording *ca.* 90% of the R-/S-1-phenylethylaminefree bases. A derivatization of these to their benzamide derivatives PhCONHCHMePh was carried out to allow chiral column chromatography and was by modification of a published procedure through reaction of the free base with benzoyl chloride (reaction in CH_2Cl_2 2 h, 0 °C with NEt_3).[55]

Chiral chromatography was carried out on the phenylamide derivatives of R- and S-1-phenylethylamines obtained from compound 7, the corresponding phenylamides of 1-phenylpropylamines derived from compound 8 and finally the doubly derivatized forms of phenylglycinol obtained from compound 9.

Accurate determination of enantiomeric excess (% ee) was carried out using CHIRALPAK® AD-H or IC columns (Daicel Chemical Industries Ltd. and Chiral Technologies, Europe) – a 5 μm silica gel coated with cellulose or amylose tris(3,5-dimethylphenyl carbamate). Elutions were 'normal phase' with either 80:20 or 85:15 mixtures of hexane:*i*-propanol.

Computation

DFT calculations on $[B\{L\text{-}Tar(NHPh)_2\}_2]^-$

Approximate starting molecular conformations were derived directly from the single crystal structure of 2 and constructed by application of 2-fold symmetry operations. Optimization and energy calculations were then carried out with 2-fold symmetry constraints (*C*2) for both "X- and Y-forms" using Becke3LYP functional[32] within Gaussian09 software package.[33] A 6-31G* basis set was used for all atoms.[56]

Conclusions

In summary the *N*,*N*′-diphenyl-L-tartramide derived bis-(tartramido)borate anions $[B\{L\text{-}Tar(NHPh)_2\}_2]^-$ have been shown to be readily prepared and crystallized. The anions have reasonably well-defined conformational preferences in several salts within the solid state. The anions in the unsolvated potassium salt 2 and its isostructural NH_4 salt 3 differ slightly from those in the methanol-solvated sodium analogue 4 through the intervention of methanol into the intra-molecular H-bonds between amide functionalities on each ligand arm. The anions in 2–4, have a tetradentate cation binding site.

Similar 'Y-shaped' anion conformations are preserved in the organoammonium salts 5–9, which indicate such anions have considerable promise for resolution. The salts isolated from several racemic amines exhibited high levels of enantiopurity. Salts from *rac*-1-phenylpropylamine (91% ee) and phenylglycinol (95% ee) were essentially directly resolved in one step. Three disorder modes H/Me site exchange, Me/Et site exchange and C–H repyramidalization at the cation sites limited the resolution efficiency in other cases. However considerable enantiopreference was found even in these solid solutions. Such promising results demonstrate the potential of bis(aryltartramido) borate anions to resolution of even challenging cases involving cations with high enantiosimilarity.

Conflicts of interest

There are no conflicts to declare.

Acknowledgements

The authors gratefully acknowledge funding of this work by the Research Grants Council of Hong Kong (grant numbers 604305, 605511 and 16306515).

References

1 R. M. Kellogg, *Acc. Chem. Res.*, 2017, **50**, 905–914; A. A. Bredkhin and Z. A. Bredikhina, *Chem. Eng. Technol.*, 2017, **40**, 1211–1220; D. Braga, L. Brammer and N. R. Champness, *CrystEngComm*, 2005, **7**, 1–19.

2 R. Siedlecka, *Tetrahedron*, 2013, **69**, 6331–6363; F. Faigl, E. Fogassy, M. Nogradi, E. Palovics and J. Schindler, *Tetrahedron: Asymmetry*, 2008, **19**, 519–536; E. Fogassy, M. Nogradi, D. Kozma, G. Egri, E. Palovics and V. Kiss, *Org. Biomol. Chem.*, 2006, **4**, 3011–3030.

3 E. L. Eliel, S. H. Wilen and L. N. Mander, *Stereochemistry of Organic Compounds*, Wiley, New York, 1994; J. Jacques, A. Collet and S. H. Wilen, *Enantiomers, Racemates and Resolution*, Wiley, New York, 1981.

4 H. Lorenz and A. Seidel-Morgenstern, *Angew. Chem., Int. Ed.*, 2014, **53**, 1218–1250; O. McConnell, A. Bach, C. Balibar, N. Byrne, Y. X. Cai, G. Carter, M. Chlenov, L. Di, K. Fan, I. Goljer, Y. N. He, D. Herold, M. Kagan, E. Kerns, F. Koehn, C. Krami, V. Marathias, B. Marquez, L. McDonald, L. Nogle, C. Petucci, G. Schlingmann, G. Tawa, M. Tischler, R. T. Williamson, A. Sutherland, W. Watts, M. Young, M. Y. Zhang, Y. R. Zhang, D. H. Zhou and D. Ho, *Chirality*, 2007, **19**, 658–682; M. Breuer, K. Ditrich, T. Habicher, B. Hauer, M. Kesseler, R. Sturmer and T. Zelinski, *Angew. Chem., Int Ed.*, 2004, **43**, 788–824; A. M. Rouhi, *Chem. Eng. News*, 2003, **81**, 56–61.

5 L. W.-Y. Wong, J. W.-H. Kan, T. Nguyen, H. H.-Y. Sung, D. Li, A. S.-F. Au Yeung, R. Sharma, Z. Lin and I. D. Williams, *Chem. Commun.*, 2015, **51**, 15760–15763.

6 L. W.-Y. Wong, J. W.-H. Kan, H. H.-Y. Sung and I. D. Williams, *Acta Crystallogr., Sect. C: Struct. Chem.*, 2017, **73**, 625–631.

7 S. H. Wilen, A. Collet and J. Jacques, *Tetrahedron*, 1977, **33**, 2725–2736.

8 K. L. Ding, Z. B. Han and Z. Wang, *Chem. – Asian J.*, 2009, **4**, 32–41; Y. Y. Liu, W. B. Li and J. L. Zhang, *Natl. Sci. Rev.*, 2017, **4**, 326; S. Chang, L. Wang and X. Lin, *Org. Biomol. Chem.*, 2018, **16**, 2239–2247.

9 F. Toda and K. Tanaka, *J. Org. Chem.*, 1988, **53**, 3607–3609; F. Toda, K. Tanaka, L. R. Nassimbeni and M. Niven, *Chem. Lett.*, 1988, 1371–1374.

10 M. G. Finn and K. B. Sharpless, *J. Am. Chem. Soc.*, 1991, **113**, 113–126; I. D. Williams, S. F. Pedersen, K. B. Sharpless and S. J. Lippard, *J. Am. Chem. Soc.*, 1984, **106**, 6430–6431.

11 A. Zalkin, D. H. Templeton and T. Ueki, *Inorg. Chem.*, 1973, **12**, 1641–1646; M. Gajhede and S. Larsen, *Acta Crystallogr., Sect. B: Struct. Sci.*, 1986, **42**, 172–180.

12 D. Horvath, G. Marcou and A. Varnek, *J. Chem. Inf. Model.*, 2013, **53**, 1543–1562; P. Willett, *Mol. Inf.*, 2014, **33**, 403–413; W.-H. Shin, X. Zhu, M. G. Bures and D. Kihara, *Molecules*, 2015, **20**, 12841–12862.

13 A. I. Kitaigorodsky, *Mixed crystals*, Springer Science & Business Media, 2012, vol. 33.

14 A. K. S. Romasanta, D. Braga, M. T. Duarte and F. Grepioni, *CrystEngComm*, 2017, **19**, 653–660; C. Brandel, S. Petit, Y. Cartigny and G. Coquerel, *Curr. Pharm. Des.*, 2016, **22**, 4929–4941; A. Bialonska and Z. Ciunik, *CrystEngComm*, 2013, **15**, 5681–5687; C. Gervais, R. F. Grimbergen, I. Markovits, G. J. Ariaans, B. Kaptein, A. Bruggink and Q. B. Broxterman, *J. Am. Chem. Soc.*, 2004, **126**, 655–662.

15 M. Balawejder, D. Kiwala, H. Lorenz, A. Seidel-Morgenstern, W. Piatkowski and D. Antos, *Cryst. Growth Des.*, 2012, **12**, 2557–2566.

16 J. M. Brunel, *Chem. Rev.*, 2007, **107**, 1–45.

17 D. R. Trivedi, A. Ballabh, P. Dastidar and B. Ganguly, *Chem. – Eur. J.*, 2004, **10**, 5311–5312.

18 Y. Yoshii, N. Hoshino, T. Takeda, H. Moritomo, J. Kawamata, T. Nakamura and T. Akutagawa, *Chem. – Eur. J.*, 2014, **20**, 16279–16285.

19 A. Jacobs, N. B. Bathori, L. R. Nassimbeni and B. K. Sebogisi, *CrystEngComm*, 2013, **15**, 931–939.

20 N. B. Bathori and L. R. Nassimbeni, *Cryst. Growth Des.*, 2012, **12**, 2501–2507.

21 C. Che, X. Dai, S. F. Mao, Y. J. Xu and Z. H. Qin, *Chin. J. Org. Chem.*, 2003, **23**, 390–392.

22 S. Larsen and H. L. Dediego, *Acta Crystallogr., Sect. B: Struct. Sci.*, 1993, **49**, 303–309; S. Larsen and H. L. Dediego, *J. Chem. Soc., Perkin Trans. 2*, 1993, 469–473; H. L. Dediego, *Acta Crystallogr., Sect. C: Cryst. Struct. Commun.*, 1994, **50**, 1995–1998; H. L. Dediego, *Acta Chem. Scand.*, 1994, **48**, 306–311.

23 D. E. Turkington, E. J. MacLean, A. J. Lough, G. Ferguson and C. Glidewell, *Acta Crystallogr., Sect. B: Struct. Sci.*, 2005, **61**, 103–114.

24 M. Pallavicini, E. Valoti, L. Villa, O. Piccolo and F. Marchetti, *Tetrahedron: Asymmetry*, 2000, **11**, 1957–1964; P. R. Anandamanoharan, P. W. Cains and A. G. Jones, *Tetrahedron: Asymmetry*, 2006, **17**, 1867–1874; K. Kodama, Y. Kimura, H. Shitara, M. Yasutake, R. Sakurai and T. Hirose, *Chirality*, 2011, **23**, 326–332.

25 P. G. Karamertzanis, P. R. Anandamanoharan, P. Fernandes, P. W. Cains, M. Vickers, D. A. Tocher, A. J. Florence and S. L. Price, *J. Phys. Chem. B*, 2007, **111**, 5326–5336; C. D. Antoniadis, E. D'Oria, P. G. Karamertzanis, D. A. Tocher, A. J. Florence, S. L. Price and A. G. Jones, *Chirality*, 2010, **22**, 447–455.

26 L. W.-Y. Wong, *PhD thesis*, Hong Kong University of Science and Technology, 2014.

27 M. Acs, E. Fogassy and F. Faigl, *Tetrahedron*, 1985, **41**, 2465–2470.

28 E. Fogassy, M. Nogradi, E. Palovics and J. Schindler, *Synthesis*, 2005, 1555–1568.

29 G. Boon, C. van Alsenoy, F. de Proft, P. Bultinck and P. Geerlings, *J. Phys. Chem. A*, 2003, **107**, 11120–11127.

30 Y. Q. Feng, Z. G. Zhong, H. W. Wang, H. T. Fan, D. Q. Bi, L. Wang, Z. Z. Xing and D. F. Qiu, *Chem. - Eur. J.*, 2017, **23**, 9962–9967.

31 L. W.-Y. Wong, A. S.-F. Au Yeung, G. S.-S. Tam, J. W.-H. Kan, F. K. Sheong, Z. Lin and I. D. Williams, *RSC Adv.*, 2018, **8**, 1451–1460.

32 A. D. Becke, *J. Chem. Phys.*, 1993, **98**, 5648–5652; C. Lee, W. Yang and R. G. Parr, *Phys. Rev. B: Condens. Matter Mater. Phys.*, 1988, **37**, 785–789; S. H. Vosko, L. Wilk and M. Nusair, *Can. J. Phys.*, 1980, **58**, 1200–1211; P. J. Stephens, F. J. Devlin, C. F. Chabalowski and M. J. Frisch, *J. Phys. Chem.*, 1994, **98**, 11623–11627.

33 M. J. Frisch, G. W. Trucks, H. B. Schlegel, G. E. Scuseria, M. A. Robb, J. R. Cheeseman, G. Scalmani, V. Barone, G. A. Petersson, H. Nakatsuji, X. Li, M. Caricato, A. Marenich, J. Bloino, B. G. Janesko, R. Gomperts, B. Mennucci, H. P. Hratchian, J. V. Ortiz, A. F. Izmaylov, J. L. Sonnenberg, D. Williams-Young, F. Ding, F. Lipparini, F. Egidi, J. Goings, B. Peng, A. Petrone, T. Henderson, D. Ranasinghe, V. G. Zakrzewski, J. Gao, N. Rega, G. Zheng, W. Liang, M. Hada, M. Ehara, K. Toyota, R. Fukuda, J. Hasegawa, M. Ishida, T. Nakajima, Y. Honda, O. Kitao, H. Nakai, T. Vreven, K. Throssell, J. A. Montgomery, Jr., J. E. Peralta, F. Ogliaro, M. Bearpark, J. J. Heyd, E. Brothers, K. N. Kudin, V. N. Staroverov, T. Keith, R. Kobayashi, J. Normand, K. Raghavachari, A. Rendell, J. C. Burant, S. S. Iyengar, J. Tomasi, M. Cossi, J. M. Millam, M. Klene, C. Adamo, R. Cammi, J. W. Ochterski, R. L. Martin, K. Morokuma, O. Farkas, J. B. Foresman and D. J. Fox, *Gaussian 09, Revision A.02*, Gaussian, Inc., Wallingford CT, 2016.

34 T. Vries, H. Wynberg, E. van Echten, J. Koek, W. ten Hoeve, R. M. Kellogg, Q. B. Broxterman, A. Minnaard, B. Kaptein, S. van der Sluis, L. A. Hulshof and J. Kooistra, *Angew. Chem., Int. Ed.*, 1998, **37**, 2349–2354; R. M. Kellogg, J. W. Nieuwenhuijzen, K. Pouwer, T. R. Vries, Q. B. Broxterman, R. F. P. Grimbergen, B. Kaptein, R. M. La Crois, E. de Wever, K. Zwaagstra and A. C. van der Laan, *Synthesis*, 2003, 1626–1638; M. R. Kellogg, B. Kaptein and T. R. Vries, *Top. Curr. Chem.*, 2007, **269**, 159–197.

35 R. J. Phipps, G. L. Hamilton and F. D. Toste, *Nat. Chem.*, 2012, **4**, 603–614.

36 J. Lacour, *C. R. Chim.*, 2010, **13**, 985–997; A. C. Veron, H. Zhang, A. Linden, F. Neusch, J. Heier, R. Hany and T. Geiger, *Org. Lett.*, 2014, **16**, 1044–1047; J. Bosson, J. Gouin and J. Lacour, *Chem. Soc. Rev.*, 2014, **43**, 2824–2840; J. Moussa, L. M. Chamoreau and H. Amouri, *Chirality*, 2013, **25**, 449–454; S. Sharma, F. Lombeck, L. Eriksson and O. Johansson, *Chem. - Eur. J.*, 2010, **16**, 7078–7081.

37 K. Kinbara, *Synlett*, 2005, 732–743; A. Ichikawa, H. Ono, T. Echigo and Y. Mikata, *CrystEngComm*, 2013, **13**, 4536–4548.

38 F. C. Ferreira, N. F. Ghazali, U. Cocchini and A. G. Livingston, *Tetrahedron: Asymmetry*, 2006, **17**, 1337–1348; H. B. Mereyala, L. Fatima and P. Pola, *Tetrahedron: Asymmetry*, 2004, **15**, 585–587.

39 C. M. Vogels and S. A. Westcott, *Chem. Soc. Rev.*, 2011, **40**, 1446–1458; D. M. Schubert, *Struct. Bonding*, 2003, **105**, 1–40.

40 W. Clegg, M. R. J. Elsegood, A. J. Scott, T. B. Marder, C. Y. Dai, N. C. Norman, N. L. Pickett and E. G. Robins, *Acta Crystallogr., Sect. C: Cryst. Struct. Commun.*, 1999, **55**, 733–739; W. Clegg, A. J. Scott, F. J. Lawlor, N. C. Norman, T. B. Marder, C. Y. Dai and P. Nguyen, *Acta Crystallogr., Sect. C: Cryst. Struct. Commun.*, 1998, **54**, 1875–1880.

41 M. Periasamy, L. Venkatraman, S. Sivakumar, N. Sampathkumar and C. R. Ramanathan, *J. Org. Chem.*, 1999, **63**, 7643–7645.

42 M. Periasamy, V. D. Rao and M. Seenivasaperumal, *Tetrahedron: Asymmetry*, 2001, **12**, 1887–1890; M. Periasamy, *Aldrichimica Acta*, 2002, **35**, 89–101.

43 S. Satishkumar and M. Periasamy, *Tetrahedron: Asymmetry*, 2006, **17**, 1116–1119; M. Periasamy, N. S. Kumar, S. Sivakumar, V. D. Rao, C. R. Ramanathan and L. Venkatraman, *J. Org. Chem.*, 2001, **66**, 3828–3833; M. Periasamy, C. R. Ramanathan and N. S. Kumar, *Tetrahedron: Asymmetry*, 1999, **10**, 2307–2310.

44 Y. Loewer, C. Weiss, A. T. Biju, R. Fröhlich and F. Glorius, *J. Org. Chem.*, 2011, **76**, 2324–2327.

45 D. Kozma, M. Acs and E. Fogassy, *Tetrahedron*, 1994, **50**, 6907–6912.

46 H. Suezawa, S. Ishihara, Y. Umezawa, S. Tsuboyama and M. Nishio, *Eur. J. Inorg. Chem.*, 2004, 4816–4822; M. Nishio, *CrystEngComm*, 2004, **6**, 130–158.

47 K. Kinbara, K. Oishi, Y. Harada and K. Saigo, *Tetrahedron*, 2000, **56**, 6651–6655; A. Ichikawa, H. Ono and Y. Mikata, *Crystals*, 2017, **7**, 263; C. Bolchi, M. Pallavicini, L. Fumagalli, N. Marchini, B. Moroni, C. Rusconi and E. Valoti, *Tetrahedron: Asymmetry*, 2005, **16**, 1639–1645.

48 W. Chen, Y. Liu and Z. Chen, *Eur. J. Org. Chem.*, 2005, 1665–1668.

49 G. M. Sheldrick, *Acta Crystallogr., Sect. C: Struct. Chem.*, 2015, **71**, 3–8; G. M. Sheldrick, *Acta Crystallogr., Sect. A: Found. Crystallogr.*, 2008, **64**, 112–122.

50 O. V. Dolomanov, L. J. Bourhis, R. J. Gildea, J. A. K. Howard and H. Puschmann, *J. Appl. Crystallogr.*, 2009, **42**, 339–341; L. J. Bourhis, O. V. Dolomanov, R. J. Gildea, J. A. K. Howard and H. Puschmann, *Acta Crystallogr., Sect. A: Found. Adv.*, 2015, **71**, 59–75.

51 A. L. Spek, *Acta Crystallogr., Sect. D: Biol. Crystallogr.*, 2009, **65**, 148–155.

52 C. F. Macrae, I. J. Bruno, J. A. Chisholm, P. R. Edgington, P. McCabe, E. Pidcock, L. Rodriguez-Monge, R. Taylor, J. van de Streek and P. A. Wood, *J. Appl. Crystallogr.*, 2008, **41**, 466–470; I. J. Bruno, J. C. Cole, P. R. Edgington, M. Kessler, C. F. Macrae, P. McCabe, J. Pearson and R. Taylor, *Acta Crystallogr., Sect. B: Struct. Sci.*, 2002, **58**, 389–397.

53 A. Altomare, G. Campi, C. Cuocci, L. Eriksson, C. Giacovazzo, A. Moliterni, R. Rizzi and P.-E. Werner, *J. Appl. Crystallogr.*, 2009, **42**, 768–775.

54 A. Boultif and D. Louër, *J. Appl. Crystallogr.*, 1991, **24**, 987–993.

55 R. Kuwano, N. Kameyama and R. Ikeda, *J. Am. Chem. Soc.*, 2011, **133**, 7312–7315.

56 V. A. Rassolov, J. A. Pople, M. A. Ratner and T. L. Windus, *J. Chem. Phys.*, 1998, **109**, 1223–1229.

